NLO production of $W^{\pm}$ and Z^0 vector bosons via hadron collisions in the frameworks of Kimber-Martin-Ryskin and Martin-Ryskin-Watt unintegrated parton distribution functions

M. Modarres,[1,*] M. R. Masouminia,[1,†] R. Aminzadeh Nik,[1] H. Hosseinkhani,[2] and N. Olanj[3]

[1]*Department of Physics, University of Tehran, 1439955961 Tehran, Iran*

[2]*Plasma and Fusion Research School, Nuclear Science and Technology Research Institute, 14395-836 Tehran, Iran*

[3]*Physics Department, Faculty of Science, Bu-AliSina University, 65178 Hamedan, Iran*

(Received 5 July 2016; published 24 October 2016)

In a series of papers, we have investigated the compatibility of the *Kimber-Martin-Ryskin* (KMR) and *Martin-Ryskin-Watt* (MRW) *unintegrated* parton distribution functions (UPDFs) as well as the description of the experimental data on the proton structure functions. The present work is a sequel to that survey, via calculation of the transverse-momentum distribution of the electroweak gauge vector bosons in the k_t-factorization scheme, by the means of the KMR, the leading-order (LO) MRW, and the next-to-leading-order (NLO) MRW UPDF, in the NLO. To this end, we have calculated and aggregated the invariant amplitudes of the corresponding *involved* diagrams in the NLO and counted the individual contributions in different frameworks. The preparation process for the UPDF utilizes the parton distribution functions of Martin *et al.*, MSTW2008-LO, MSTW2008-NLO, MMHT2014-LO, and MMHT2014-NLO, as the inputs. Afterward, the results have been analyzed against each other as well as the existing experimental data, i.e., D0, CDF, ATLAS, and CMS collaborations. Our calculations show excellent agreement with the experiment data. It is, however, interesting to point out that the calculation using the KMR framework illustrates a stronger agreement with the experimental data, despite the fact that the LO MRW and the NLO MRW formalisms employ a better theoretical description of the Dokshitzer-Gribov-Lipatov-Altarelli-Parisi evolution equation. This is of course due to the use of the different implementation of the angular ordering constraint in the KMR approach, which automatically includes the resummation of $\ln(1/x)$, Balitski-Fadin-Kuraev-Lipatov logarithms, in the LO Dokshitzer-Gribov-Lipatov-Altarelli-Parisi evolution equation.

DOI: 10.1103/PhysRevD.94.074035

I. INTRODUCTION

In recent years, new discoveries have been made at many high-energy particle physics laboratories, including the LHC, concerning physics within the boundaries of the Standard Model and beyond, as the consequence of pushing the maximum energy of the experiments to new limits. Today, many of these laboratories use parton distribution functions (PDFs) to describe and analyze their extracted data from the deep inelastic QCD collisions. These scale-dependent functions are the solutions of the Dokshitzer-Gribov-Lipatov-Altarelli-Parisi (DGLAP) evolution equations [1–4],

$$\frac{da(x,Q^2)}{d\log(Q^2)}=\frac{\alpha_s(Q^2)}{2\pi}\sum_{b=q,g}\left[\int_x^1 dz P_{ab}(z) b\left(\frac{x}{z},Q^2\right)-a(x,Q^2)\int_0^1 dz z P_{ba}(z)\right], \tag{1}$$

where $a(x,Q^2)$ can be either the distribution function of the quarks, $xq(x,Q^2)$, or that of the gluons, $xg(x,Q^2)$, with x being the fraction of the longitudinal momentum of the parent hadron (the Bjorken variable). The terms on the right-hand side of the equation (1) correspond to the real emission and the virtual contributions, respectively. The scale Q^2 is an ultraviolet cutoff, related to the virtuality of the exchanged particle during the deep inelastic scattering (DIS). $P_{ab}(z)$ are the splitting functions of the respective partons which account for the probability of a parton $a(x'',Q^2)$ emerging from a parent parton $b(x',Q^2)$ through $z=x''/x'$.

*Corresponding author.
mmodares@ut.ac.ir

†Visitor research fellow to the Institute of Nuclear Physics, Polish Academy of Science, Krakow, Poland.

The DGLAP evolution equation, however, is based on the *strong ordering* assumption, which systematically neglects the transverse momentum of the emitted partons along the evolution ladder. It has been repeatedly hinted that undermining the contributions coming from the transverse momentum of the partons may severely harm the precision of the calculations, especially in the high-energy processes in the small-x region; see, for example, Refs. [5–9]. This signaled the necessity of introducing some transverse momentum-dependent (TMD) PDF, initially through the Ciafaloni-Catani-Fiorani-Marchesini (CCFM) equation [10–14],

$$f(x,k_t^2,Q^2) = f_0(x,k_t^2,Q^2) + \int_x^1 dz \int \frac{dq^2}{q^2}\Theta(Q-zq)\Delta_S(Q,zq) \times P(z,\bar{\alpha}_s(k_t^2))f\left(\frac{x}{z},|\mathbf{k_t}+(1-z)\mathbf{q}|^2,q^2\right). \quad (2)$$

The $\Theta(Q-zq)$ implies a physical condition, enforcing the increase of the angle of the emission of the gluons in successive radiations along the evolution chain. This condition which is usually referred to as the angular ordering constraint (AOC), is due to the coherent radiation of the gluons. The Sudakov form factor, $\Delta_S(Q,q)$, gives the probability of evolving from a scale q to a scale Q, without any partons emission, and can be defined as

$$\Delta_S(Q,q) = \exp\left(-\bar{\alpha_s}\int_{q^2}^{Q^2}\frac{dk^2}{k^2}\int_0^1 dz'\frac{1}{(1-z)}\right), \quad (3)$$

with $\bar{\alpha}_s = 3\alpha_s/\pi$. In Eq. (2), $f(x,k_t^2,\mu^2)$ is the double-scaled CCFM TMD PDF, which in addition to the x and Q depends on the transverse momentum of the incoming partons, k_t. It has been shown (see Ref. [15]) that in the proper boundaries, the CCFM equation will reduced to the conventional DGLAP and Balitski-Fadin-Kuraev-Lipatov (BFKL) equations, [16–20].

The procedure of solving the CCFM equation is mathematically involved and unrealistically time consuming, since it includes contemplating iterative integral equations with many terms. On the other hand, the main feature of the CCFM equation, i.e., the AOC, can be exclusively used for the gluon evolution, and therefore this process is incapable of producing a convincing quark contribution. To overcome these obstacles, Martin *et al.* have introduced the k_t-factorization framework and developed the Kimber-Martin-Ryskin (KMR) and the Martin-Ryskin-Watt (MRW) approaches [5,6], both of which are constructed around the LO DGLAP evolution equations and modified with the different visualizations of the angular ordering constraint. The frameworks of KMR and MRW in the leading order (LO) and next-to-leading order (NLO) have been investigated intensely in the recent years; see Refs. [21–28].

Although Martin *et al.* have developed the MRW formalism as an improvement to the KMR approach, by correcting the use of the AOC, limiting its effect only on the diagonal splitting functions and extending the range of their calculations into the NLO via introducing the NLO MRW scheme, it appears that the KMR approach, as an effective model, is more successful in producing a realistic theory in order to describe the experiment. We are therefore eager to expand our investigation regarding the merits and shortcomings of these frameworks into the calculation of the inclusive cross sections of production of the electroweak gauge bosons in high-energy hadronic collisions.

The process of the production of the massive gauge vector bosons, $W^{\pm}$ and Z^0, has always been of extreme theoretical and experimental interest, since it can provide invaluable information about the nature of both the electroweak and the strong interactions, setting a benchmark for testing the validity of the experiments and establishing a firm base for testing new theoretical frameworks; see Refs. [29–42]. It is not, however, straightforward to describe the transverse-momentum distributions of the electroweak bosons produced in hadron-hadron collisions, since the usual collinear factorization approach in the LO neglects the transverse-momentum dependency of the incoming partons and therefore predicts a vanishing transverse momentum for the product. Consequently, initial-state QCD radiation is necessary to generate the k_t distributions. On the other hand, in this approximation, calculations for differential cross sections of the $W^{\pm}$ and Z^0 production diverge logarithmically in the NLO limit for the $k_t \ll M_{W,Z}$ (which is the main region of interest), due to the soft gluon emission. So, one requires a resummation to obtain a finite k_t distribution.

In the present work, we tend to calculate the k_t distributions of the cross section of production of the $W^{\pm}$ and Z^0 using the NLO level diagrams and the LO and NLO unintegrated PDF (UPDF) of the KMR and the MRW frameworks. The UPDF will be prepared in their proper k_t-factorization schemes using the PDF of MSTW2008-LO, MSTW2008-NLO, MMHT2014-LO, and MMHT2014-NLO [43–46]. Such calculations have been previously carried out using LO matrix elements of quark-antiquark annihilation cross section and doubly unintegrated parton distribution functions (DUPDFs) in

the framework of (k_t, z) factorization [9] and in a semi-NLO approach, using a mixture of LO and NLO matrix elements for the involved processes in addition to a variety of TMD PDF; see Ref. [40]. To improve these approximations and at the same time test the functionality of the KMR and the MRW UPDF, we have calculated the NLO ladder diagrams for $g + g \to W^{\pm}/Z^0 + q + q'$, $q + g \to W^{\pm}/Z^0 + q' + g$, and $q + q' \to W^{\pm}/Z^0 + g + g$, utilizing a physical gauge for the gluons. In this way, at the price performing long and complicated calculations, we will demonstrate that with the use of the UPDF in the NLO calculations one can extract an excellent description of the experimental data of the D0, CDF, ATLAS, and CMS collaborations [29–39], as well as other works given here, regarding the transverse-momentum distributions of the $W^{\pm}$ and Z^0 boson [40–42].

In what follows, first, a brief introduction to the concept of k_t factorization will be presented, and the respective formalisms for the KMR and the MRW frameworks will be derived in Sec. II. Section III contains a comprehensive description over the utilities and means for the calculation of the k_t-dependent cross section of the production of the $W^{\pm}$ and Z^0 gauge vector bosons in a hadron-hadron (or hadron-antihadron) deep inelastic collision. The necessary numerical analysis will be presented in Sec. IV, after which a thoroughgoing conclusion will follow in Sec. V.

II. k_t-FACTORIZATION SCHEME

A parton entering the subprocess at the top of the evolution ladder has non-negligible transverse momentum. However, it is customary to use the PDF of the DGLAP or the BFKL evolution equations to describe such partons, despite the fact that these density functions intrinsically carry no k_t dependency. To include the contributions coming from the transverse-momentum distributions of the partons, one can either use the solutions of the CCFM evolution equation or unify the BFKL and the DGLAP evolution equations to form a properly tuned k_t-dependent framework [47,48]. Nevertheless, given the mathematical complexity of these schemes, it is not desirable to use them in the task of computing the DIS cross sections. Another way is to convolute the single-scaled solutions of the DGLAP evolution equation and insert the required k_t dependency via the process of k_t factorization (for a complete description, see Ref. [8]).

Thus, one may define the UPDF, $f_a(x, k_t^2, \mu^2)$, in the k_t-factorization scheme, through the normalization relation

$$a(x, \mu^2) = \int^{\mu^2} \frac{dk_t^2}{k_t^2} f_a(x, k_t^2, \mu^2), \tag{4}$$

where $a(x, \mu^2)$ are the solutions of the DGLAP equation and stand for either $xq(x, \mu^2)$ or $xg(x, \mu^2)$. The procedure of deriving a direct expansion for $f_a(x, k_t^2, \mu^2)$, in terms of the PDF is straightforward. Yet, exposing the resulting prescriptions to the different visualizations of the AOC will produce different UPDF, namely, the KMR, the LO MRW, and the NLO MRW frameworks. In what follows, we will describe these frameworks in detail.

A. KMR framework

Starting form the DGLAP equation in the leading order, Eq. (1), and using the unregulated LO DGLAP splitting kernels, $P_{ab}(z)$ [49], Kimber *et al.* introduced an infrared cutoff, Δ, as a visualization of the AOC [50],

$$\Theta(\theta - \theta') \Rightarrow \mu > \frac{z k_t}{(1-z)} \Rightarrow \Delta = \frac{k_t}{\mu + k_t}.$$

Limiting the upper boundary on z integration by Δ excludes $z = 1$ form the integral equation and automatically prevents facing the soft gluon singularities arising from the $1/(1-z)$ terms in the splitting functions. Additionally, they factorized the virtual contributions from the DGLAP equations, by defining a virtual (loop) contribution as

$$T_a(k_t^2, \mu^2) = \exp\left(- \int_{k_t^2}^{\mu^2} \frac{\alpha_S(k^2)}{2\pi} \frac{dk^2}{k^2} \sum_{b=q,g} \int_0^{1-\Delta} dz' P_{ab}^{(\mathrm{LO})}(z') \right), \tag{5}$$

with

$$T_a(\mu^2, \mu^2) = 1$$

as an appropriated form of the Sudakov form factor (3). Afterward, the double-scaled KMR UPDF are defined as follows:

$$f_a(x, k_t^2, \mu^2) = T_a(k_t^2, \mu^2) \sum_{b=q,g} \left[\frac{\alpha_S(k_t^2)}{2\pi} \int_x^{1-\Delta} dz P_{ab}^{(\mathrm{LO})}(z) b\left(\frac{x}{z}, k_t^2\right) \right]. \tag{6}$$

According to the above formulation, only at the last step of the evolution does the dependence on the second scale, μ, get introduced into the UPDF. The required PDF is provided as input, using the libraries MSTW2008 [43–45] and MMHT2014 [46], where the calculation of the single-scaled functions have been carried out using the DIS data on the F_2 structure function of the proton. T_a are considered to be unity for $k_t > \mu$. This constraint and its interpretation in terms of the strong ordering condition gives the KMR approach a smooth behavior over the small-x region, which is generally governed by the BFKL evolution equation.

B. LO MRW framework

In coordination with the theory of gluonic coherent radiation, it has been pointed out that the AOC in the KMR formalism should only act on the terms including the on-shell gluon emissions, i.e., the diagonal splitting functions $P_{qq}(z)$ and $P_{gg}(z)$. Therefore, Martin *et al.* defined the LO MRW UPDF as the correction to the KMR framework [6],

$$f_q^{\mathrm{LO}}(x,k_t^2,\mu^2) = T_q(k_t^2,\mu^2)\frac{\alpha_S(k_t^2)}{2\pi}\int_x^1 dz\left[P_{qq}^{(\mathrm{LO})}(z)\frac{x}{z}q\left(\frac{x}{z},k_t^2\right)\Theta\left(\frac{\mu}{\mu+k_t}-z\right)+P_{qg}^{(\mathrm{LO})}(z)\frac{x}{z}g\left(\frac{x}{z},k_t^2\right)\right], \tag{7}$$

with

$$T_q(k_t^2,\mu^2) = \exp\left(-\int_{k_t^2}^{\mu^2}\frac{\alpha_S(k^2)}{2\pi}\frac{dk^2}{k^2}\int_0^{z_{\max}} dz' P_{qq}^{(\mathrm{LO})}(z')\right) \tag{8}$$

for the quarks and

$$f_g^{\mathrm{LO}}(x,k_t^2,\mu^2) = T_g(k_t^2,\mu^2)\frac{\alpha_S(k_t^2)}{2\pi}\int_x^1 dz\left[P_{gq}^{(\mathrm{LO})}(z)\sum_q\frac{x}{z}q\left(\frac{x}{z},k_t^2\right)+P_{gg}^{(\mathrm{LO})}(z)\frac{x}{z}g\left(\frac{x}{z},k_t^2\right)\Theta\left(\frac{\mu}{\mu+k_t}-z\right)\right], \tag{9}$$

with

$$T_g(k_t^2,\mu^2) = \exp\left(-\int_{k_t^2}^{\mu^2}\frac{\alpha_S(k^2)}{2\pi}\frac{dk^2}{k^2}\left[\int_{z_{\min}}^{z_{\max}} dz' z' P_{qq}^{(\mathrm{LO})}(z')+n_f\int_0^1 dz' P_{qg}^{(\mathrm{LO})}(z')\right]\right), \tag{10}$$

for the gluons. In Eqs. (8) and (10), $z_{\max} = 1 - z_{\min} = \mu/(\mu + k_t)$ [49]. The UPDF of KMR and MRW to a good approximation include the main kinematical effects involved in the DIS processes. One should note that the particular form of the AOC in the KMR formalism, despite being of the LO, includes some contributions from the NLO sector, whereas in the case of the MRW framework, these contributions must be inserted separately.

C. NLO MRW framework

The expansions of the LO MRW formalism into the NLO region can be achieved through the definitions

$$f_a^{\mathrm{NLO}}(x,k_t^2,\mu^2) = \int_x^1 dz T_a\left(k^2=\frac{k_t^2}{(1-z)},\mu^2\right)\frac{\alpha_S(k^2)}{2\pi}\sum_{b=q,g}\tilde{P}_{ab}^{(\mathrm{LO+NLO})}(z)\times b^{\mathrm{NLO}}\left(\frac{x}{z},k^2\right)\Theta\left(1-z-\frac{k_t^2}{\mu^2}\right), \tag{11}$$

with the NLO splitting functions being defined as

$$\tilde{P}_{ab}^{(\mathrm{LO+NLO})}(z) = \tilde{P}_{ab}^{(\mathrm{LO})}(z)+\frac{\alpha_S}{2\pi}\tilde{P}_{ab}^{(\mathrm{NLO})}(z), \tag{12}$$

and

$$\tilde{P}_{ab}^{(i)}(z) = P_{ab}^i(z)-\Theta(z-(1-\Delta))\delta_{ab}F_{ab}^i P_{ab}(z), \tag{13}$$

where $i = 0,\ 1$ stand for LO and NLO, respectively. The reader can find a comprehensive description of the NLO splitting functions in Refs. [6,51]. We must, however, emphasize that, contrary to the KMR and the LO MRW frameworks, the AOC is being introduced into the NLO MRW formalism via the $\Theta(z-(1-\Delta))$

constraint, in the "extended" splitting function. Now, Δ can be defined as

$$\Delta = \frac{k\sqrt{1-z}}{k\sqrt{1-z}+\mu}.$$

The NLO corrections introduced into this framework are the collection of the NLO PDF, the NLO splitting functions and the constraint $\Theta(1-z-k_t^2/\mu^2)$. Nevertheless, it has been shown that using only the LO part of the extended splitting function, instead of the complete definition of Eq. (12), would result in reasonable accuracy in computation of the NLO MRW UPDF [6]. Additionally, the Sudakov form factors in this framework are defined as

$$T_q(k^2,\mu^2) = \exp\left(-\int_{k^2}^{\mu^2}\frac{\alpha_S(q^2)}{2\pi}\frac{dq^2}{q^2}\int_0^1 dz' z'[\tilde{P}_{qq}^{(0+1)}(z')+\tilde{P}_{gq}^{(0+1)}(z')]\right), \tag{14}$$

$$T_g(k^2,\mu^2) = \exp\left(-\int_{k^2}^{\mu^2}\frac{\alpha_S(q^2)}{2\pi}\frac{dq^2}{q^2}\int_0^1 dz' z'[\tilde{P}_{gg}^{(0+1)}(z')+2n_f\tilde{P}_{qg}^{(0+1)}(z')]\right). \tag{15}$$

Each of these UPDFs, the KMR, LO, and NLO MRW, can be used to identify the probability of finding a parton of a given flavor, with the fraction x of longitudinal momentum of the parent hadron, the transverse momentum k_t in the scale μ at the semihard level of a particular DIS process. In the following section, we will describe the cross section of the production of the $W^{\pm}$ and Z^0 bosons with the help of our UPDF.

III. PRODUCTION OF $W^{\pm}$ AND Z^0 IN THE k_t FACTORIZATION

By definition, the total cross section for a deep hadronic collision, $\sigma_{\text{Hadron-Hadron}}$, can be written in terms of its possible partonic constituents. Utilizing the UPDF as density functions for the involved partons, one may write $\sigma_{\text{Hadron-Hadron}}$ in the form

$$\sigma_{\text{Hadron-Hadron}} = \sum_{a_1,a_2=q,g}\int_0^1\frac{dx_1}{x_1}\int_0^1\frac{dx_2}{x_2}\int_0^\infty\frac{dk_{1,t}^2}{k_{1,t}^2}\int_0^\infty\frac{dk_{2,t}^2}{k_{2,t}^2} f_{a_1}(x_1,k_{1,t}^2,\mu_1^2) f_{a_2}(x_2,k_{2,t}^2,\mu_2^2)\hat{\sigma}_{a_1a_2}(x_1,k_{1,t}^2,\mu_1^2;x_2,k_{2,t}^2,\mu_2^2), \tag{16}$$

where a_1 and a_2 are the incoming partons into the semihard process from the first and the second hadrons, respectively. $\hat{\sigma}_{a_1a_2}$ are the corresponding partonic cross sections, which can be defined separately as

$$d\hat{\sigma}_{a_1a_2} = \frac{d\phi_{a_1a_2}}{F_{a_1a_2}}|\mathcal{M}_{a_1a_2}|^2. \tag{17}$$

$d\phi_{a_1a_2}$ and $F_{a_1a_2}$ are the multiparticle phase space and the flux factor, respectively, and can be defined according to the specifications of the partonic process,

$$d\phi_{a_1a_2} = \prod_i\frac{d^3p_i}{2E_i}\delta^{(4)}\left(\sum p_{\text{in}}-\sum p_{\text{out}}\right), \tag{18}$$

$$F_{a_1a_2} = x_1x_2s, \tag{19}$$

with the s being the center-of-mass energy squared,

$$s = (P_1+P_2)^2 = 2P_1.P_2.$$

P_1 and P_2 are the 4-momenta of the incoming protons, and since we are working in the infinite-momentum frame, it is safe to neglect their masses. $d\phi_{a_1a_2}$ can be characterized in terms of transverse momenta of the product particles, $p_{i,t}$; their rapidities, y_i; and the azimuthal angles of the emissions, φ_i:

$$\frac{d^3p_i}{2E_i} = \frac{\pi}{2}dp_{i,t}^2dy_i\frac{d\varphi_i}{2\pi}. \tag{20}$$

In Eq. (17), $\mathcal{M}_{a_1a_2}$ are the matrix elements of the partonic diagrams which are involved in the production of the final results. To calculate these quantities, one must first understand the exact kinematics that rule over the corresponding partonic processes.

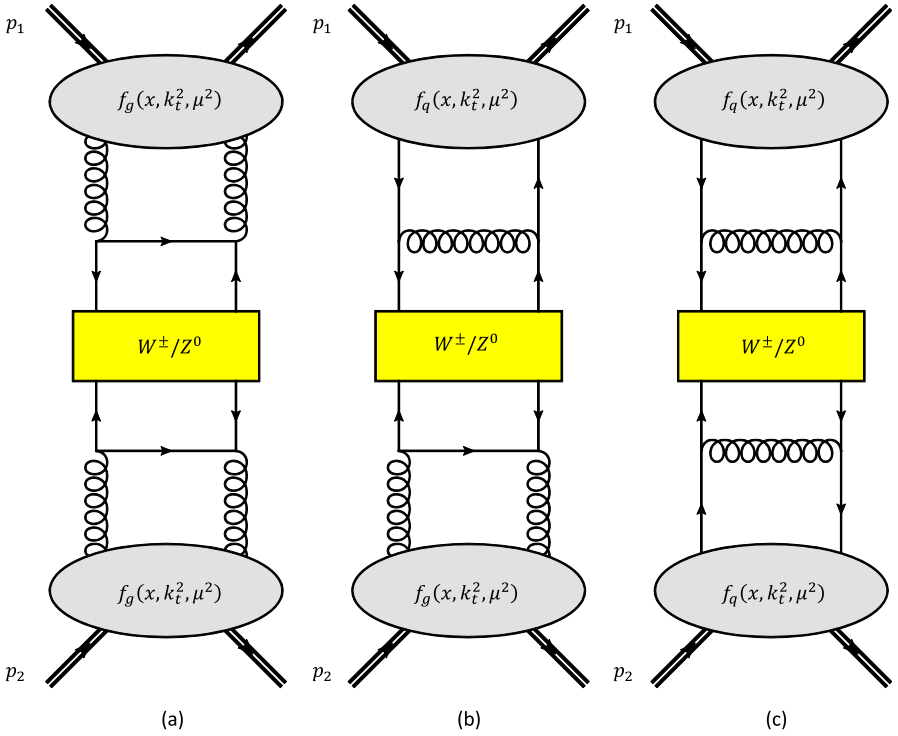

FIG. 1. The NLO ladder-type diagrams for the production of $W^\pm$ and Z^0 in the k_t-factorization framework. The $f_g(x,k_t^2,\mu^2)$ and $f_q(x,k_t^2,\mu^2)$ represent the corresponding UPDF in the KMR, the LO-MRW, or the NLO-MRW framework, i.e., Eqs. (6), (7), (9), and (11).

Figure 1 illustrates the ladder-type NLO diagrams that one has to consider, counting the contributions coming from $g+g\to W^\pm/Z^0+q+q'$, $q+g\to W^\pm/Z^0+q'+g$, and $q+q'\to W^\pm/Z^0+g+g$ as shown in Fig. 1, panels (a), (b), and (c), respectively. The kinematics and calculations of this type of invariant amplitudes have been discussed extensively in Refs. [9,40,41]. We have followed the same approach, obtaining the $dk_{i,t}^2/k_{i,t}^2$ terms only from the ladder-type diagrams and not from the interference (i.e., the nonladder) diagrams, using a physical gauge for the gluons, where only the two transverse polarizations propagate,

$$d_{\mu\nu}(k)=-g_{\mu\nu}+\frac{k_\mu n_\nu+n_\mu k_\nu}{k.n}. \tag{21}$$

$n=x_1P_1+x_2P_2$ is the gauge-fixing vector. Choosing such a gauge condition ensures that the $dk_{i,t}^2/k_{i,t}^2$ terms are being obtained from the ladder-type diagrams on both sides of the subprocesses. In the case of hadron-hadron collisions, one might expect that neglecting the contributions coming from the nonladder diagrams, i.e., the diagrams where the production of the electroweak bosons is a byproduct of the hadronic collision (see Ref. [41]), would have a numerical effect on the results. Nevertheless, employing the gauge choice (21), one finds out that the contribution from the "unfactorizable" nonladder diagrams vanishes.

In the proton-antiproton center-of-mass frame, we can write the kinematics

$$P_1=\frac{\sqrt{s}}{2}(1,0,0,1),\qquad P_2=\frac{\sqrt{s}}{2}(1,0,0,-1),$$
$$\mathbf{k}_i=x_i\mathbf{P}_i+\mathbf{k}_{i,\perp},\qquad k_{i,\perp}^2=-k_{i,t}^2,\qquad i=1,2, \tag{22}$$

where the k_i, $i=1,2$ are the 4-momenta of the partons that enter the semihard process. Afterward, it is possible to write the law of the transverse-momentum conservation for the partonic process,

$$\mathbf{k}_{1,\perp}+\mathbf{k}_{2,\perp}=\mathbf{p}_{1,\perp}+\mathbf{p}_{2,\perp}+\mathbf{p}_\perp, \tag{23}$$

with $\mathbf{p}_\perp$ being the transverse momentum of the produced vector boson. Additionally, defining the transverse mass of the produced virtual partons, $m_{i,t}=\sqrt{m_i^2+p_i^2}$, we can write

$$x_1=(m_{1,t}e^{y_1}+m_{2,t}e^{y_2}+m_{W/Z,t}e^{y_{W/Z}})/\sqrt{s},$$
$$x_2=(m_{1,t}e^{-y_1}+m_{2,t}e^{-y_2}+m_{W/Z,t}e^{-y_{W/Z}})/\sqrt{s}. \tag{24}$$

Now, using the above equations, one can derive the following equation for the total cross section of the production of the $W^\pm$ and Z^0 bosons in the framework of k_t factorization,

$$\sigma(P+\bar{P}\to W^{\pm}/Z^0+X)=\sum_{a_i,b_i=q,g}\int\frac{dk^2_{a_1,t}}{k^2_{a_1,t}}\frac{dk^2_{a_2,t}}{k^2_{a_2,t}}dp^2_{b_1,t}dp^2_{b_2,t}dy_1dy_2dy_{W/Z}\frac{d\varphi_{a_1}}{2\pi}\frac{d\varphi_{a_2}}{2\pi}\frac{d\varphi_{b_1}}{2\pi}\frac{d\varphi_{b_2}}{2\pi}$$
$$\times\frac{|\mathcal{M}(a_1+a_2\to W^{\pm}/Z^0+b_1+b_2)|^2}{256\pi^3(x_1x_2s)^2}f_{a_1}(x_1,k^2_{a_1,t},\mu^2)f_{a_2}(x_2,k^2_{a_2,t},\mu^2). \quad (25)$$

Note that the integration boundaries for $dk^2_{i,t}/k^2_{i,t}$ are $(0,\infty)$. One may introduce an upper limit for these, say $k_{i,\max}$, several times larger than the scale μ, without any noticeable consequences. Yet, for $k_t<\mu_0$ with $\mu_0=1$ GeV, i.e., for the nonperturbative region, it is imperative to decide how to validate our UPDF. A natural choice would be to fulfill the requirement that

$$\lim_{k^2_{a_i,t}\to 0} f_{a_i}(x_i,k^2_{a_i,t},\mu^2)\sim k^2_{a_i,t},$$

and therefore we can safely choose the following approximation for the nonperturbative region:

$$f_{a_i}(x_i,k^2_{a_i,t}<\mu_0^2,\mu^2)=\frac{k^2_{a_i,t}}{\mu_0^2}a_i(x_i,\mu_0^2)T_{a_i}(\mu_0^2,\mu^2). \quad (26)$$

In the next section, we will introduce some of the numerical methods that have been used for the calculation of the $\sigma(P+\bar{P}\to W^{\pm}/Z^0+X)$ (25) using the UPDF of KMR and MRW. It is expected that through considering NLO processes for this computation the results will have a better agreement with the existing experimental data, in comparison with the previous calculations.

IV. NUMERICAL ANALYSIS

The main challenge one must face, in the computations of the total cross section of a hadron-hadron collision in the NLO, is the extremely complex calculations required for extracting the invariant amplitudes in a set of $2\to 3$ NLO Feynman diagrams. Each of our processes, $g+g\to W^{\pm}/Z^0+q+q'$, $q+g\to W^{\pm}/Z^0+q'+g$, and $q+q'\to W^{\pm}/Z^0+g+g$, includes a number of different configurations; see Fig. 2. This is when we filter out the nonladder diagrams, with our choice of the gauge condition on the gluon polarization (21). Writing the analytic expressions of the $\mathcal{M}_{ab}$ for theses diagrams is rather straightforward; see Appendix A.

However, since the incoming and the outgoing quarks are off shell, and we do not neglect their transverse momenta, their on-shell spin density matrices have to be

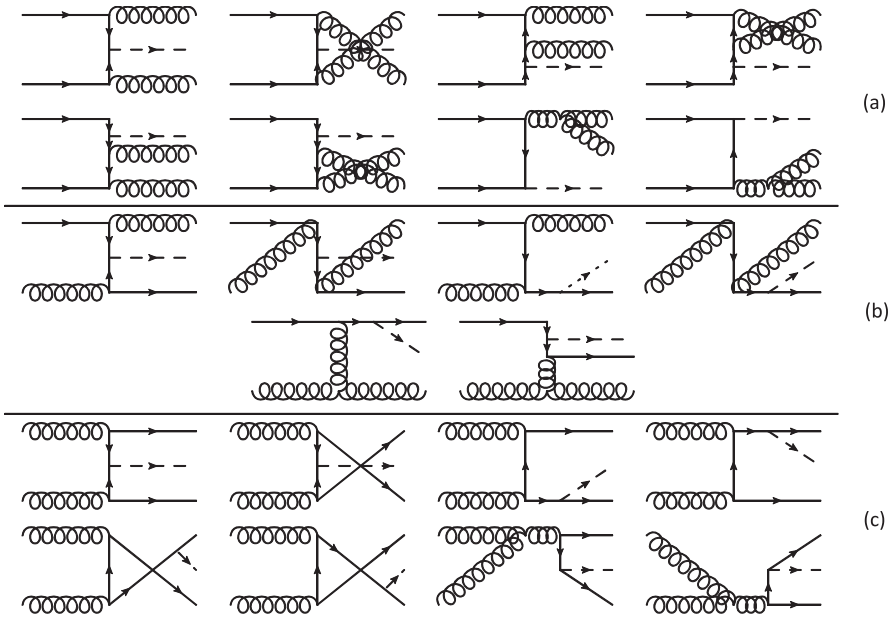

FIG. 2. The individual contributions into the matrix elements of the partonic scattering. The diagrams in the panel (a) correspond to the $q+\bar{q}'\to W^{\pm}/Z^0+g+g$ subprocess, panel (b) corresponds to the $q+g\to W^{\pm}/Z^0+q+g$ subprocess, and panel (c) corresponds to the $g+g\to W^{\pm}/Z^0+q+\bar{q}'$ subprocess. It should be pointed out that one may find additional non-ladder-type diagrams which contribute to these matrix elements. We have eliminated these undesirable contributions using our choice of the gluon gauge, Eq. (21).

replaced with a more complicated expression. To do this, one can extend the original expressions, according to an approximation proposed in Refs. [52,53], through converting the off-shell quark lines to the internal lines via replacing the spinorial elements of the incoming and the outgoing partons. Following this idea, we replace the incoming proton with a quark with the momentum p and the mass m which radiates a photon or a gluon and turns into an off-shell quark with the momentum k. Therefore, the corresponding matrix element for such quarks can be written as

$$|\mathcal{M}|^2 \sim \mathrm{Tr}\left(\Gamma_\mu \frac{\hat{k}+m}{k^2-m^2}\gamma^\nu u(p)\bar{u}(p)\gamma_\nu \frac{\hat{k}+m}{k^2-m^2}\Gamma^\mu\right),$$

where Γ_μ represents the rest of the original matrix element. Now, the expression presented between Γ_μ and Γ^μ is considered to be the off-shell quark spin density matrix. Using the on-shell identity

$$\sum u(p)\bar{u}(p) = \hat{p} + m,$$

and after performing some Dirac algebra at the $m \to 0$ limit, one simply arrives at the following expression:

$$|\mathcal{M}|^2 \sim \frac{2}{k^4}\,\mathrm{Tr}(\Gamma_\mu[k^2\hat{p} - 2(p\cdot k)\hat{k}]\Gamma^\mu).$$

Afterward, imposing the Sudakov decomposition $k = xp + k_t$ with $k^2 = k_t^2 = -\mathbf{k}_t^2$, one derives

$$|\mathcal{M}|^2 \sim \frac{2}{xk_t^2}\,\mathrm{Tr}(\Gamma_\mu x\hat{p}\Gamma^\mu). \tag{27}$$

Thus, with the above replacement, the negative light-cone momentum fractions of the incoming partons have been neglected. $x\hat{p}$ in this equation represents the properly normalized off-shell spin density matrix. Additionally, the coupling vertices of the off-shell gluons to quarks must be modified with the eikonal vertex (i.e., the BFKL prescription; see Ref. [41]). Therefore, in the case of initial off-shell gluons, we impose the so-called nonsense polarization condition, i.e.,

$$\epsilon_\mu(k_i) = \frac{2k_{i,\mu}}{\sqrt{s}},$$

which results into the following normalization identity:

$$\sum \epsilon_\mu(k_i)\epsilon_\nu^*(k_i) = \frac{k_{i,\mu}k_{i,\nu}}{k_{i,t}^2}.$$

We can calculate the evolution of the traces of the matrix elements with the help of the algebraic manipulation system FORM [54]. Also, the method of orthogonal amplitudes, see Ref. [41], can be used to further simplify the results.

The numerical computation of Eq. (25) has been carried out using the VEGAS algorithm in the Monte Carlo integration. To do this, we have selected the hard scale of the UPDF to be equal to the transverse mass of the produced gauge vector boson:

$$\mu = (m_{W/Z}^2 + p_{W/Z,t}^2)^{\frac{1}{2}}.$$

Mathematically speaking, the upper bound on the transverse-momentum integrations of the master equation (25) should be infinity. However, since the UPDFs of KMR and MRW tend to quickly vanish in the $k_t \gg \mu$ domain, one can safely introduce an ultraviolet cutoff for these integrations. By convention, this cutoff is considered to be at $k_{i,\max} = p_{i,\max} = 4\mu$. Nevertheless, given that μ depends on the transverse momentum of the produced boson ($p_{W/Z,t}$) and its mass, it would be sufficient to set $k_{i,\max} = p_{i,\max} = 4\mu_{\max}$, with

$$\mu_{\max} = (m_{W/Z}^2 + p_{t,\max}^2)^{\frac{1}{2}}.$$

One can easily confirm that further domains have no contribution to our results. Also, it is satisfactory to bound the rapidity integrations to $[-10, 10]$, since $0 \le x \le 1$ and according to Eq. (24) a further domain has no contribution into our results. The choice of the above hard scale is reasonable for the production of W and Z bosons, as has been discussed in Ref. [41].

As a final note, we should make it clear that in Ref. [40] the calculation of the transverse-momentum distribution for the production of the W and Z bosons has been carried out, using the aggregated contributions of the following subprocesses:

(a) The NLO $g + g \to W/Z + q + \bar{q}$ partonic process, using the unintegrated gluon distributions of the CCFM and the LO MRW formalisms, accounting for the production of the bosons accompanied by (at least) two distinct jets.
(b) The LO $q + g \to W/Z + \bar{q}$ partonic process, with the density function of the incoming quarks and gluons being defined in the collinear [Glück-Reya-Vogt (GRV) or MSTW] and the k_t-factorization (the CCFM and the LO MRW) formalisms, respectively. This corresponds to the $p + \bar{p} \to W/Z + \mathrm{jet} + X$ cross section.
(c) The LO $q + \bar{q} \to W/Z$ partonic process, from the collinear approximation, assuming that the incoming particles are valence quarks (or valence antiquarks).

The above partonic processes (a, b, and c) obviously neglect some of the NLO contributions (in the b and c cases), namely, the shares of the nonvalence quarks along the chain of evolution. Additionally, assuming the nonzero transverse momentum for the valence quarks in the infinite-momentum frame is to some extent unacceptable, since, in

the absence of any extra structure, the intrinsic transverse momenta of the valence quarks should not be enough for producing the W/Z bosons with relatively large p_t. In the present work, we have upgraded the partonic processes of the b and c cases with their NLO counterparts, i.e., $q^* + g^* \to W/Z + q + g$ and $q^* + \bar{q}^* \to W/Z + g + g$ subprocesses. So, we are able to use the UPDF of the k_t factorization for the incoming quarks and gluons to insert the transverse-momentum dependency of the produced bosons and at the same time avoid overcounting. Furthermore, the problem of separating the W/Z + single-jet and the W/Z + double-jet cross sections will reduce to inserting the correct physical constraints on the dynamics of these processes, e.g., via inserting some transverse-momentum cuts for the produced jets, using the anti-k_t algorithm; see Ref. [55]. Nevertheless, since we are interested in calculating the inclusive cross section for the production of the W/Z bosons, inserting such constraints is unnecessary.

One should note that the partonic subprocesses that contribute to the production of Z^0 bosons are the same in either $p - p$ or $p - \bar{p}$ collisions. The crucial difference arises from the configuration of the distribution functions of the incoming partons. For example, in the $p - p$ case, one has to consider a $f_q \times f_{\bar{q}}$ setup, while in the $p - \bar{p}$ case, $f_q \times f_q$ would be sufficient since $f_q^p = f_{\bar{q}}^{\bar{p}}$.

V. RESULTS, DISCUSSIONS, AND CONCLUSIONS

Using the theory and the notions of the previous sections, one can calculate the production rate of the $W^{\pm}$ and Z^0 gauge vector bosons for the center-of-mass energy of 1.8 TeV. The PDFs of Martin *et al.* [43–46], MSTW2008 and MMHT2014, are used as the input functions to feed Eqs. (6), (7), (9), and (11). The results are the double-scale UPDF in the KMR, the LO MRW, and the NLO MRW schemes. These UPDFs are in turn substituted into Eq. (25) to construct the W/Z cross sections in their respective frameworks. Since we intend to compare our calculations to the $W^{\pm} \to l^{\pm} + \nu$ and $Z \to l^+ + l^-$ decays, we should multiply our theoretical output by the relevant branching fractions, i.e., $f(W^{\pm} \to l^{\pm} + \nu) = 0.1075$ and $f(Z \to l^+ + l^-) = 0.03366$ [56]. Thus, Figs. 3 and 4 present the reader with a comparison between the different contributions into the differential cross sections of the $W^{\pm}$ and Z^0 vs their transverse momentum (k_t) in the KMR scheme. The main contributions to the production of the $W^{\pm}$ are those involving $u \to W + d$ and $c \to W + s$ vertices. Other production vertices have been calculated and proven to be negligible compared to these main contributions (nevertheless, for the sake of completeness, we have included every single share, no matter how small they are in the total contributions; see Figs. 5 and 6, where the individual contributions of each of the production vertices in the partonic subprocesses for the production of $W^{\pm}$ and Z^0 have been depicted clearly, in the framework of KMR for $E_{\mathrm{CM}} = 1.8$ TeV). In the case of Z^0 production, the main vertices are $u \to Z + u$, $d \to Z + d$, $c \to Z + c$, and $s \to Z + s$. In both cases, one can recognize the different behavior of various partonic subprocesses. As expected, the

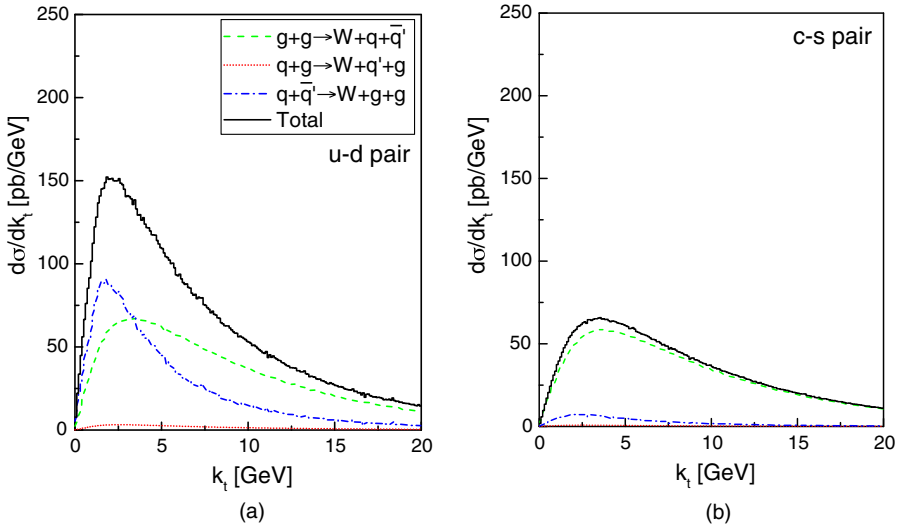

FIG. 3. The differential cross section of the productions of $W^{\pm}$ bosons in a DIS at $E_{\mathrm{CM}} = 1.8$ TeV, against the transverse-momentum distribution of the produced particle. The panels (a) and (b) illustrate the up-down and charm-strange contributions, respectively. The contribution of each partonic subprocess is singled out: the green-dashed histogram is for $g + g \to W^{\pm} + q + \bar{q}'$, the red-dotted histogram is for $q + g \to W^{\pm} + q' + g$, and the blue-dashed-dotted histogram is for $q + \bar{q}' \to W^{\pm} + g + g$. The black full histogram is the total contribution of the given quark pairs. The histograms are produced using the KMR UPDF with the PDF of MSTW2008.

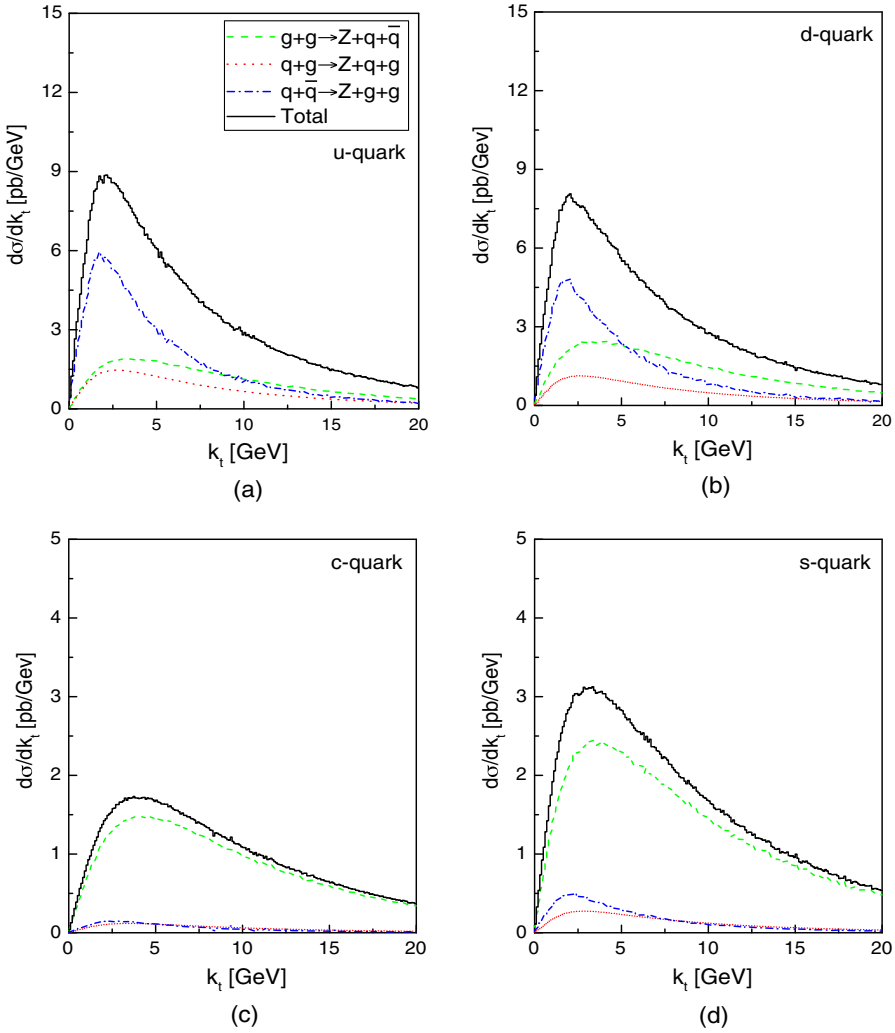

FIG. 4. The differential cross section of the productions of Z^0 boson in a DIS at $E_{\mathrm{CM}} = 1.8$ TeV, against the transverse-momentum distribution of the produced particle. The contributions of the up and the down quarks [the panels (a) and (b), respectively] and the lightest sea quarks [the panel (c) for the charm quark and the panel (d) for the strange quark]. The green-dashed histogram is for $g + g \to Z^0 + q + \bar{q}$, the red-dotted histogram is for $q + g \to Z^0 + q + g$, and the blue-dashed-dotted histogram is for $q + \bar{q} \to Z^0 + g + g$. The black full histogram is the total contribution of the given quarks. The data are produced using the KMR UPDF, with the PDF of MSTW2008.

contributions of the $g + g \to W/Z + q + \bar{q}'$ in all of the diagrams are similar, and even (roughly) of the same size, since they only depend on the behavior of the gluon density. On the other hand, the contribution coming from the $q + \bar{q}' \to W/Z + g + g$ differs from one production vertex to another, mimicking the differences between the quark densities of different flavors and going from the high contributions of the up and down quarks to small contributions of the charm and strange and even negligible contributions of the top and bottom quarks. Additionally, one notices the smallness of the $q + g \to W/Z + q' + g$ contributions. This is also anticipated, since the incoming gluon could (with a relatively large probability) decay into a quark-antiquark pair that does not have the right flavor to form a production vertex with considerable contribution.

Figures 7 and 8 illustrate a complete comparison between the results of the calculation of the production of the electroweak gauge vector bosons in the frameworks of KMR, LO MRW, and NLO MRW with each other and with the experimental data of the D0 and CDF collaborations, Refs. [31,32,34–37]. The results in the KMR framework have excellent agreement with the experimental data, both in the $W^{\pm}$ and Z^0 productions. The LO MRW scheme behaves similarly compared to the KMR framework yet has a noticeably shorter peak, especially in the case of Z^0. This is due the different visualization of the AOC between these two frameworks; see the Sec. III.

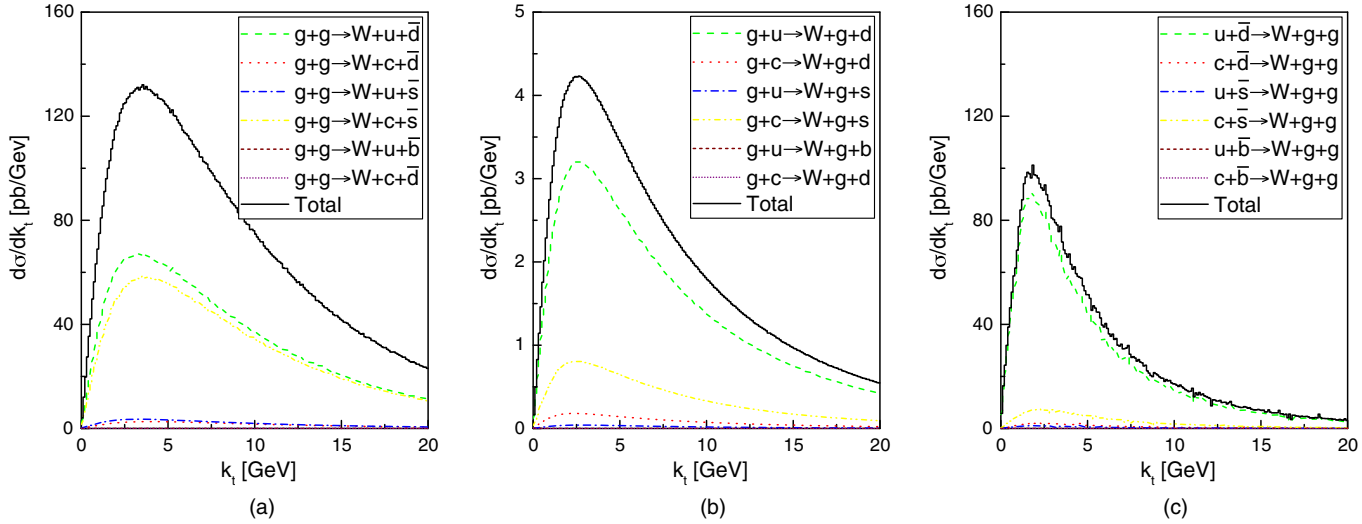

FIG. 5. The contributions of the individual partonic subprocesses to the differential cross section of the productions of $W^{\pm}$ bosons in a DIS at $E_{\mathrm{CM}} = 1.8$ TeV vs the transverse-momentum distribution of the produced particle. The panels (a), (b), and (c) correspond to the $g + g \to W^{\pm} + q + \bar{q}'$, $q + \bar{q}' \to W^{\pm} + g + g$ and $g + q \to W^{\pm} + g + q'$ sub-processes, respectively. The data have been obtained using the UPDF of KMR, with the PDF of MSTW2008.

Meanwhile, the results in the NLO MRW scheme are unexpectedly unable to describe the experiment data. This is related to the conditions in which the AOC has been imposed in this framework. The $\theta(1 - z - k_t^2/\mu^2)$ constraint gives the parton distributions of the NLO MRW, a sharp descent to zero at $k_t \to \mu$, and returns a vanishing contribution for the better part of the transverse-momentum integration in Eq. (25). Consequently, the overall value of the differential cross sections of the $W^{\pm}$ and Z^0 production in this framework reduces dramatically, as is apparent Figs. 7 and 8. Overall and as has been stated elsewhere (see, for example, Refs. [27,28]), the results in the KMR scheme seemingly have better agreement with the experiment. This is to some extent ironic, since the LO and the NLO MRW formalisms are developed as extensions and improvements to the KMR approach and are more compatible with the DGLAP evolution equation.

Such comparisons can also be made for the larger values of k_t, see Figs. 9 and 10, where the production rates of the electroweak gauge bosons are plotted against their

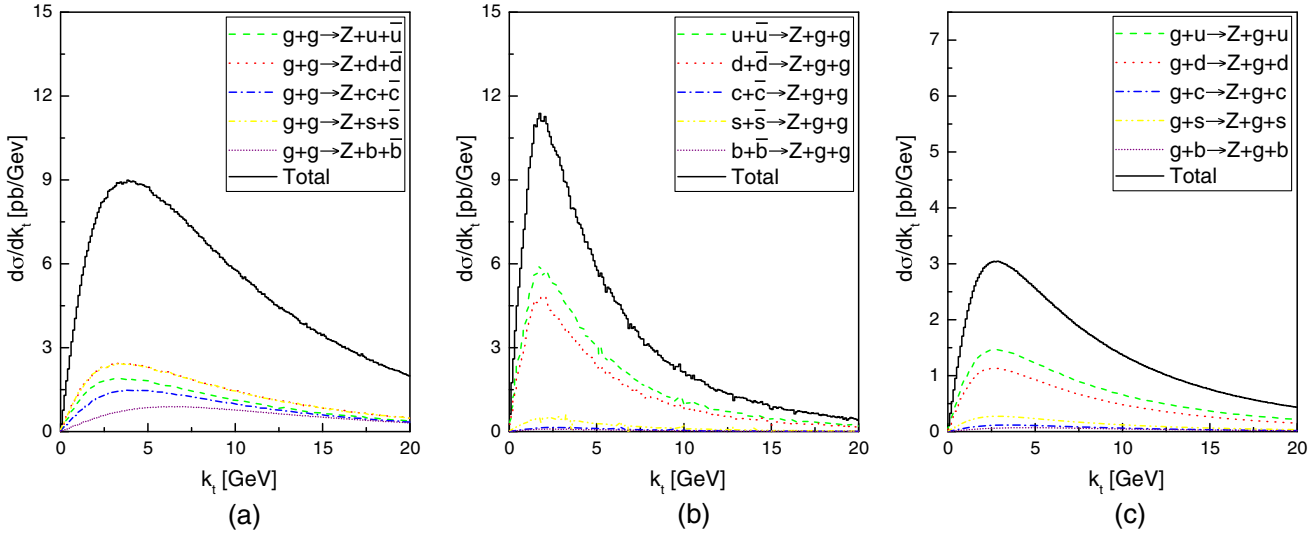

FIG. 6. The contributions of the individual partonic subprocesses into the differential cross section of the productions of Z^0 bosons in a DIS at $E_{\mathrm{CM}} = 1.8$ TeV vs the transverse-momentum distribution of the produced particle. The notions of the diagrams are the same as in Fig. 5.

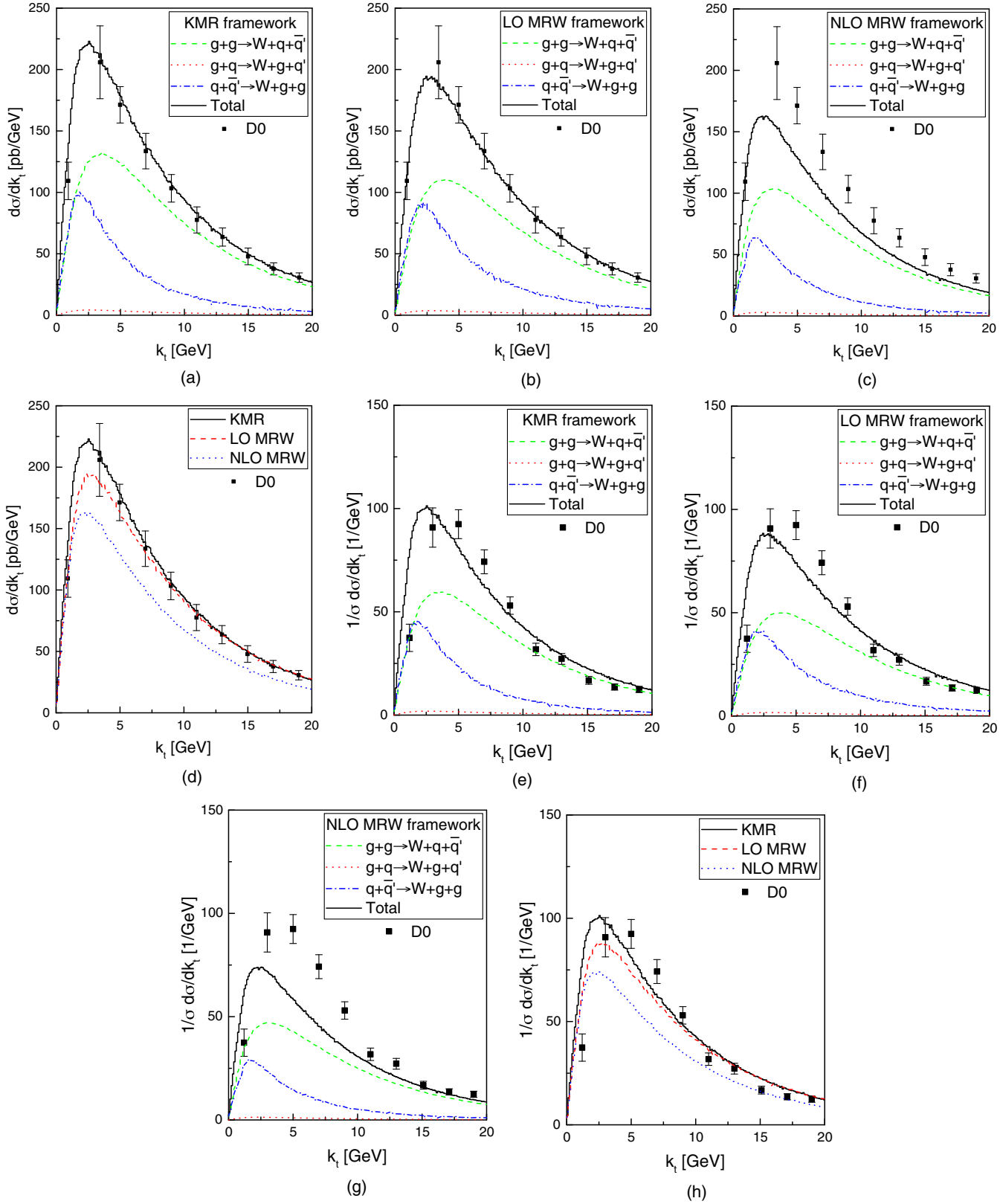

FIG. 7. The comparison of the differential cross section of the $W^{\pm}$ production in the NLO in the KMR [panel (a)], LO MRW [panel (b)], and NLO MRW [panel (c)] frameworks. Panel (d) illustrates this comparison with the help of experimental data of the D0 Collaboration, Ref. [37]. Panels (e), (f), and (g) are the same values, but this time they divided by the total cross sections in their respective frameworks and compared to an older set of data points from the D0 Collaboration, [34]. Again, an overall comparison with the experiment is presented in panel (h). To perform these calculations, we have utilized the PDF of MSTW2008.

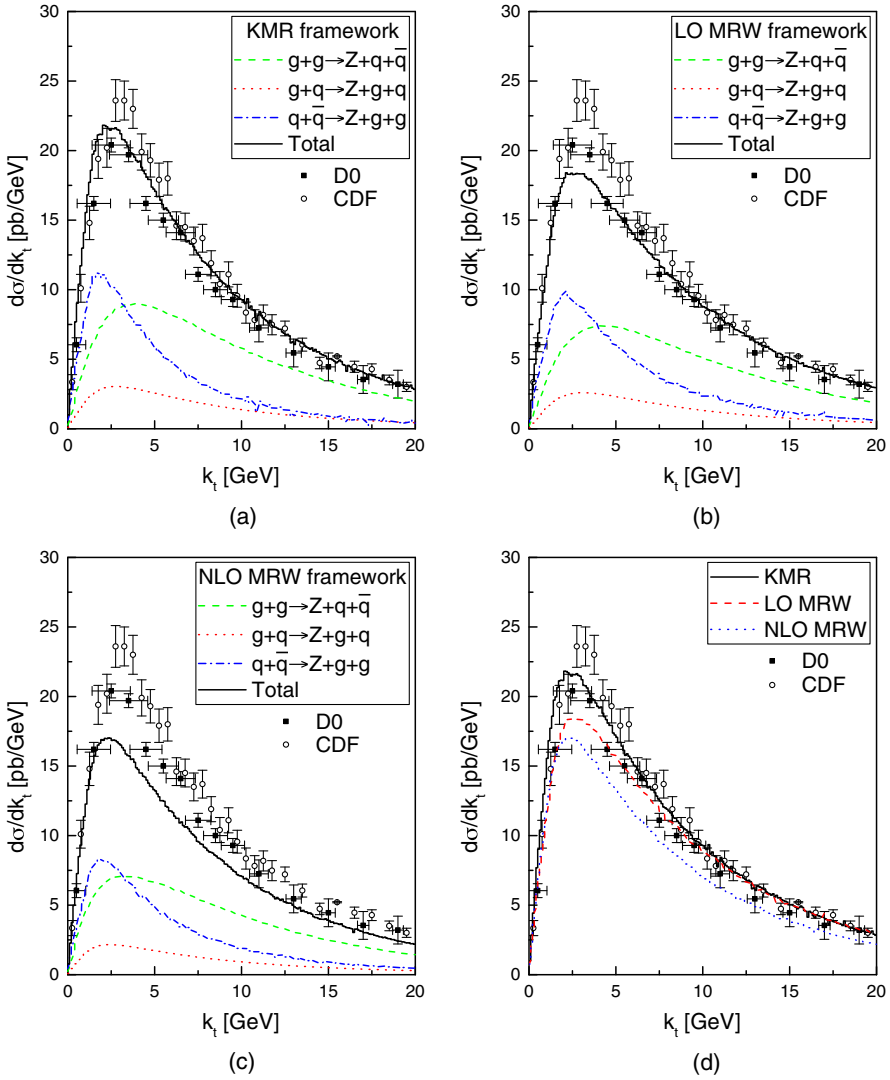

FIG. 8. The comparison of the differential cross section of the Z^0 production in the NLO in the KMR [panel (a)], LO MRW [panel (b)], and NLO MRW [panel (c)] frameworks. Panel (d) illustrates this comparison with the help of the experimental data of D0 and CDF collaborations, Refs. [32,34].

transverse momentum for $k_t < 200$ GeV. The diagrams include the calculations of $d\sigma_{W/Z}/dk_t$ and $1/\sigma_W d\sigma_W/dk_t$, and the comparisons are made with the help of the data from the D0 Collaboration, Refs. [34,37]. Of course, since the data points have small values and large errors and because of the closeness of the results in different frameworks, one cannot stress over the superiority of any of the approaches. Yet, our previous conclusion about the validity of the KMR UPDF and the shortcomings of the NLO MRW UPDF holds. Another interesting observation is that in the large k_t, where because of the smallness of the results the higher-order corrections become important, the calculations in the KMR approach start to separate from the LO MRW and behave similarly to the NLO MRW. The reason is that the inclusion of the *nondiagonal* splitting functions in the domain of the AOC introduces some corrections from the NLO region. Additionally, one notices that the contribution coming from the $q + q' \to W^{\pm} + g + g$ in the NLO evaluations considerably deviates from the similar behavior of its respective counterparts. This of course rooted in the evolution of the NLO quark densities in this framework; see Ref. [49].

Recently, Martin *et al.* have updated their PDF libraries [46]. Figures 11 and 12 demonstrate the differences between the cross sections of the production of the W/Z vector bosons in the KMR framework, using the (older) MSTW2008 and the (newer) MMHT2014 PDF. One notices that using either of these PDFs as input for our UPDF produces a negligible difference.

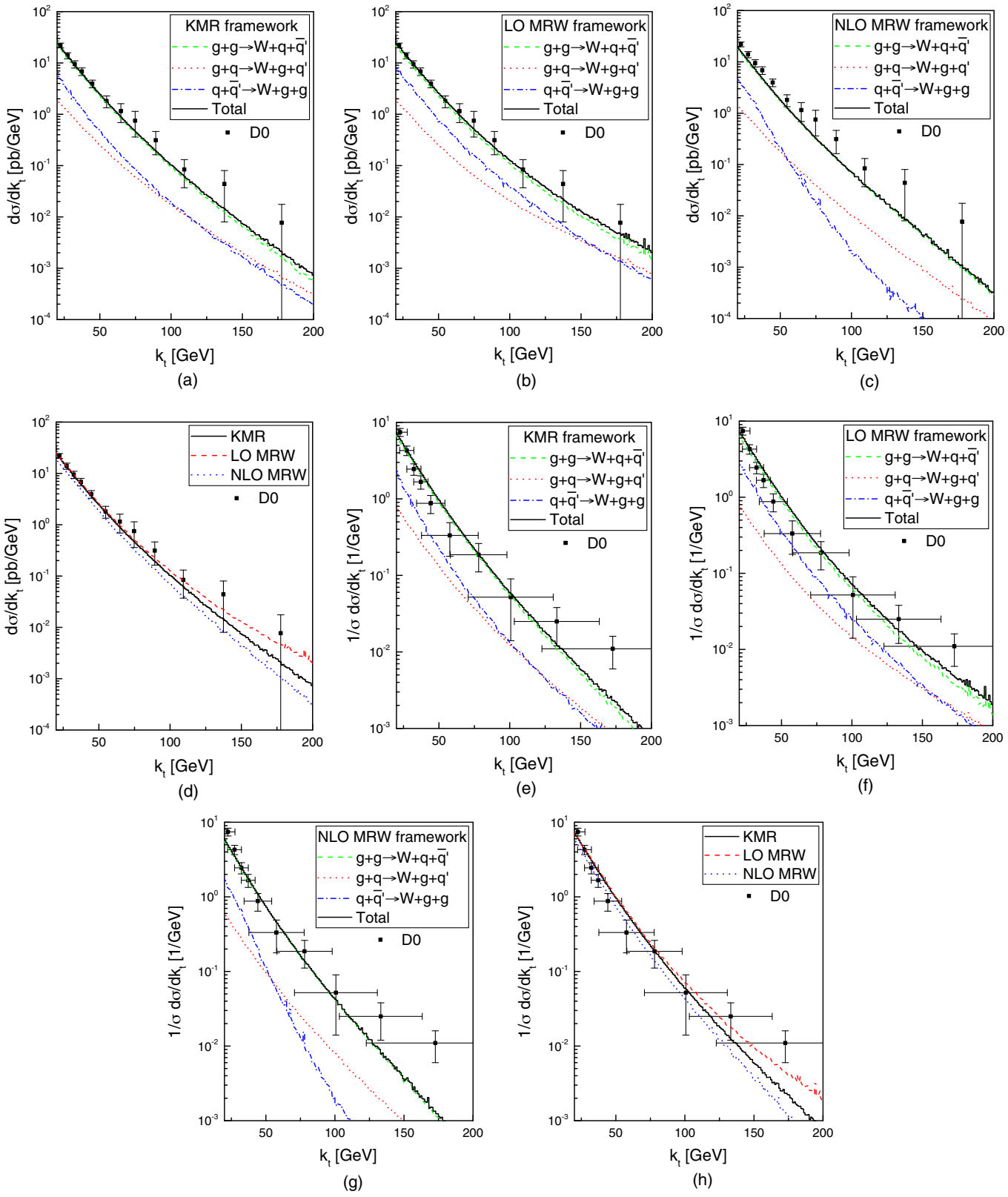

FIG. 9. The production rate of the $W^{\pm}$ boson in $E_{\mathrm{CM}} = 1.8$ TeV. The labels (a), (b), and (c) compare the contributions of the individual subprocesses in their respective frameworks. The total values of differential cross section in these frameworks are subjected to a comparison with the data of the D0 Collaboration [37] separately, in label (d). This very same notion is also presented in labels (e) through (f), where the $1/\sigma d\sigma/dk_t$ histograms are compared with each other and with the data from Ref. [34].

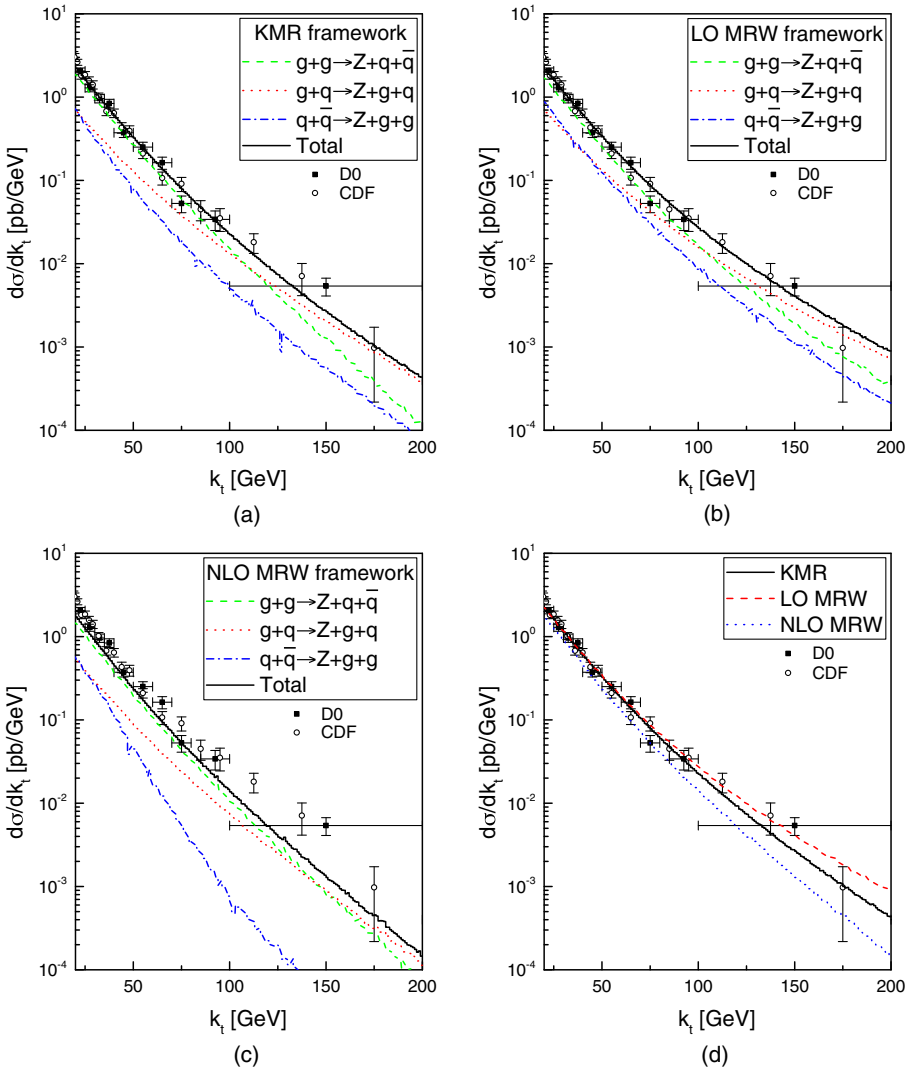

FIG. 10. The production rate of the Z^0 boson in $E_{\mathrm{CM}} = 1.8$ TeV. The notions of the diagrams are the same as in Fig. 9.

Figures 13 and 14 present an interesting comparison between the experimental data and the results of the different approximations in the calculation of the production of the electroweak gauge vector bosons. In addition to our calculations in the KMR and the MRW UPDF in the LO and the NLO approximations, the results coming from the CCFM TMD PDF (Ref. [40]), from the *doublly unintegrated* parton distributions (see Ref. [9]), and from the *collinear* frameworks are included in these diagrams. The CCFM results are calculated as the sum of $g+g \to W/Z+q+\bar{q}'$, $g+q \to W/Z+q'$, and $q+q \to W/Z$ subprocesses. The DUPDF results are in the $(k_t - z)$-factorization framework, utilizing a $q+q \to W/Z$ "effective" production vertex. Furthermore, to calculate the differential cross section of the W/Z production in the collinear approximation, one has to ignore the transverse-momentum integrations in Eq. (25) and replace the UPDF with the unpolarized parton distributions of MSTW2008, MMHT2014, or GRV2009 [57–59]:

$$\sigma(P+\bar{P} \to W^{\pm}/Z^0+X) = \sum_{a_i,b_i=q,g} \int dp^2_{b_1,t} dp^2_{b_2,t} dy_1 dy_2 dy_{W/Z} \frac{d\varphi_{b_1}}{2\pi} \frac{d\varphi_{b_2}}{2\pi} \times \frac{|\mathcal{M}(a_1+a_2 \to W/Z+b_1+b_2)|^2}{256\pi^3 (x_1 x_2 s)^2} a_1(x_1,\mu^2) a_2(x_2,\mu^2). \quad (28)$$

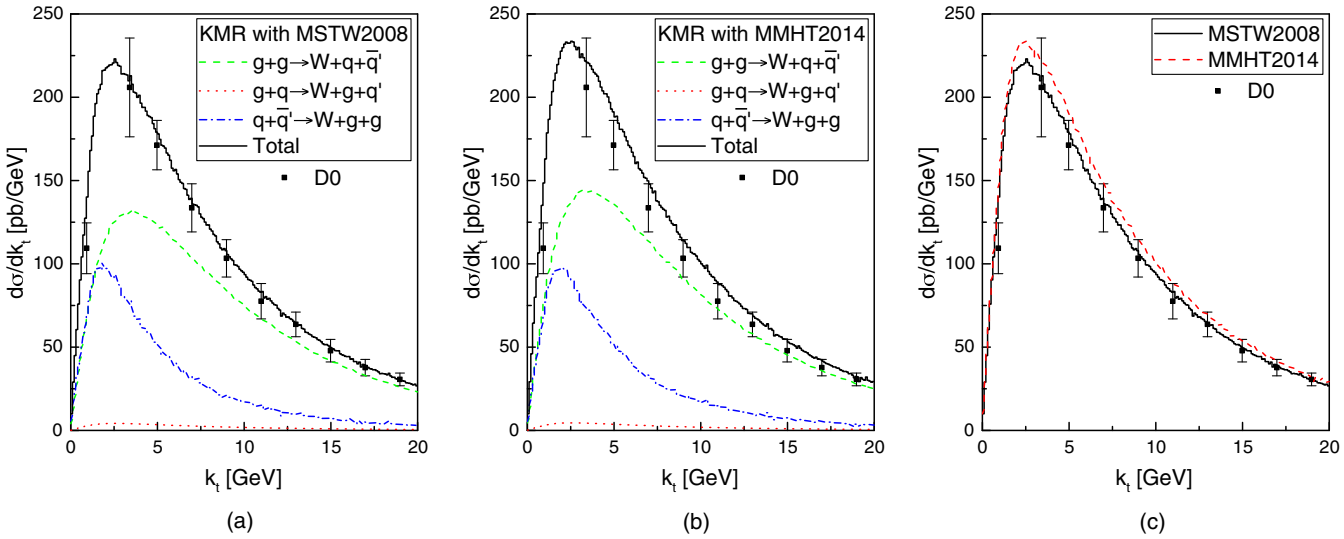

FIG. 11. Comparison of the differential cross section of the $W^{\pm}$ production, using the UPDF of KMR, prepared with the PDF of MSTW2008 [label (a)] and MMHT2014 [label (b)]. Label (c) shows their difference relative to the experimental data of the D0 Collaboration, Ref. [37].

Note that the curves that are labeled as LO collinear have been calculated in Ref. [40], utilizing the LO quark-antiquark annihilation matrix elements [see Fig. 5 and Eqs. (A3) and (A4) of Ref. [40], bearing in minding that Eq. (A1) of this reference is to some extent misleading in this regard]. To include the transverse dependency of the produced gauge vector bosons, Eq. (4) has been embedded into Eq. (28). Nevertheless, since the LO matrix elements are independent of the transverse momenta of the incoming partons, the result should in theory be unchanged (and still in the collinear approximation). In addition to their LO level precision, the shortcomings of such computations compared to the experimental data are also a consequence of the discrepancy that naturally accompanies the identity (4); see Ref. [5].

The reader should notice that the results of our computations in the NLO regime, as expected, have a better behavior toward describing the experimental data, both in the $W^{\pm}$ and Z^0 cases, since they descend with a shallow steep, compared to the results calculated in other schemes.

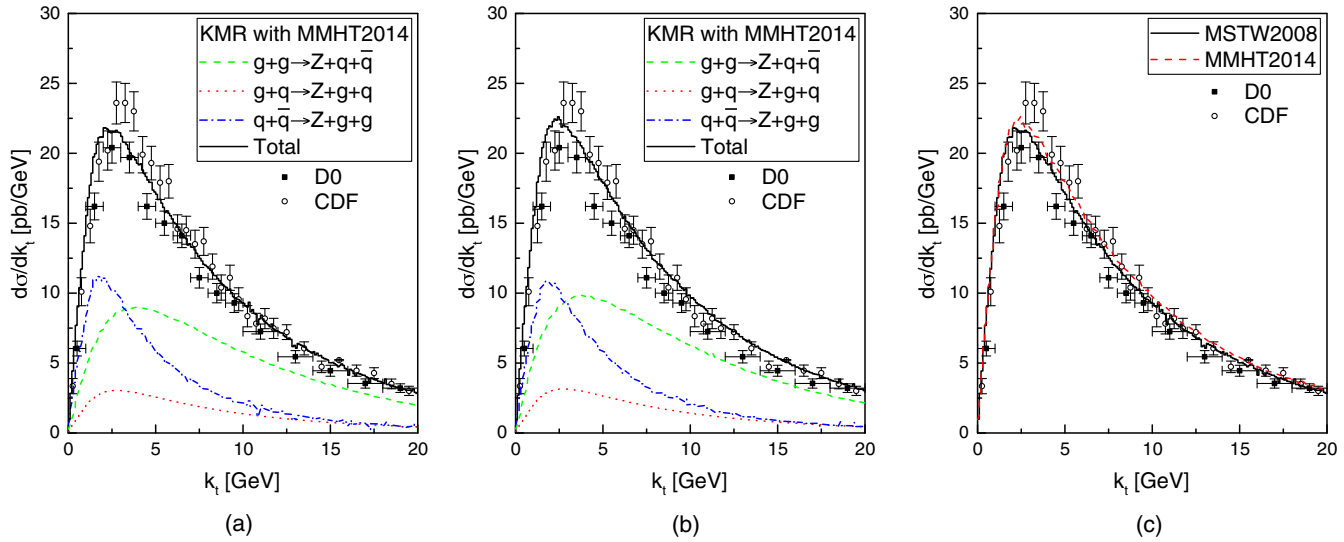

FIG. 12. Comparison of the differential cross section of the Z^0 production, using the UPDF of KMR, prepared with the PDF of MSTW2008 [label (a)] and MMHT2014 [label (b)]. Label (c) shows their difference relative to the experimental data of the D0 and CDF collaborations, Refs. [32,34].

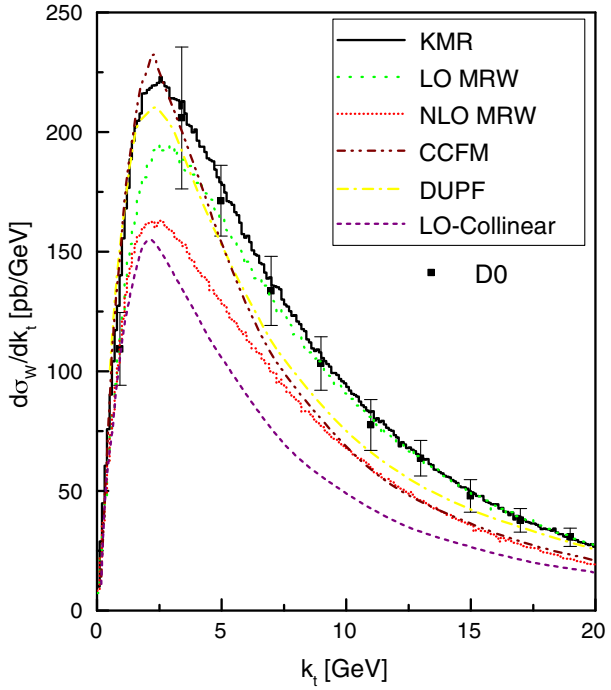

FIG. 13. The differential cross section of the production of the $W^{\pm}$, calculated in different frameworks, against the transverse momentum of the produced gauge boson at $E_{\mathrm{CM}} = 1.8$ TeV. The notions of the histograms are as follows: the continuous black histogram represents the calculation in using the KMR UPDF, the dotted green histogram is prepared in the LO MRW framework, and the short-dotted red line is prepared in the NLO MRW. To perform these calculations, we have utilized the PDF of MSTW2008. The brown dot-dot-dashed histogram is produced using the CCFM TMD PDF (Ref. [40]). The yellow dotted-dashed histogram is calculated, utilizing the doubly DUPDF in the framework of $(k_t - z)$ factorization [9]. The purple short-dashed histogram is calculated in the collinear framework.

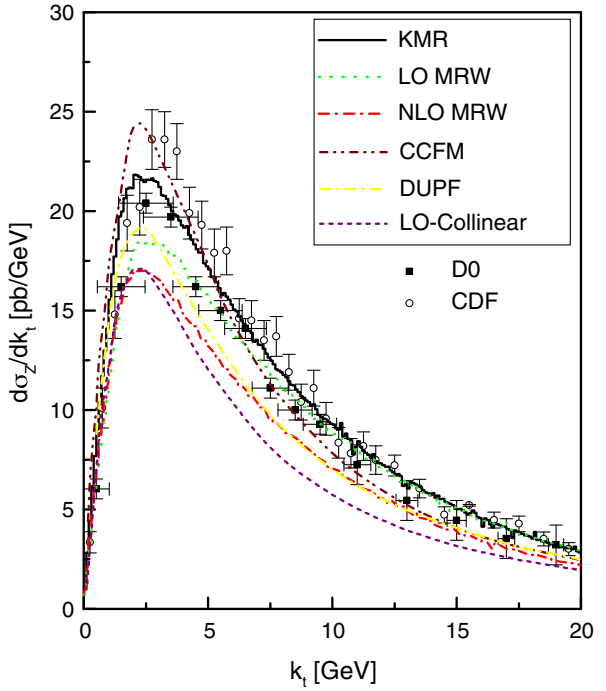

FIG. 14. The differential cross section of the production of the Z^0, calculated in different frameworks, against the transverse momentum of the produced gauge boson at $E_{\mathrm{CM}} = 1.8$ TeV. The notions of the histograms are the same as in Fig. 13.

This is in part because the NLO evaluations are inherently more accurate. Yet, most of the credit goes to the precision of the utilized UPDF. Again, the KMR framework in the NLO calculations offers the best description of the experiment.

Additionally, it is possible to compare our presumed frameworks through the calculation of the total cross section of the $W^{\pm}$ and Z^0 production with respect to the center-of-mass energy of the hadronic collision, i.e., Figs. 15 and 16. Following our previous pattern, the results of both the KMR and the LO MRW frameworks show a good level of compatibility with the experimental data. On the other hand, since the NLO MRW framework has failed to describe the data, we have excluded its contributions here, to save some computation time.

Finally, it has been brought to our attention that the ATLAS and CMS collaborations have recently published some data regarding the production of the Z^0 gauge vector boson in the LHC for $E_{\mathrm{CM}} = 8$ TeV [38,39]. In the above calculations, the rapidity of the produced boson has been separated in equally spaced rapidity sectors within $0 < |y_Z| < 2.4$ domain. In Fig. 17, we have addressed the above observations, using our NLO framework and utilizing the UPDF of KMR, since we have already established the superiority of this scheme in describing the experiment. The individual contributions from the partonic subprocesses are presented, and the total values of (single and double) differential cross sections are subjected to comparison with the data of the ATLAS and CMS collaborations. We should mention that the recent theoretical next-to-next-to-leading-order (NNLO) QCD calculation, i.e., Ref. [42], have been very successful in describing these experimental measurements with respect to the present formalism.

Unfortunately, performing these calculations is extremely time consuming, and the existing data points are not plentiful or accurate enough to let us make a decisive statement about the superiority regarding any of our presumed frameworks. Nevertheless, considering these comparisons, it is apparent that the KMR UPDFs in the framework of k_t factorization, despite their misalignments with the theory of the DGLAP evolution equation and the physics of the successive gluon radiations, as an effective theory, proposes the best option to describe the deep inelastic QCD events. However, until further phenomenological analysis, such a claim remains an educated speculation.

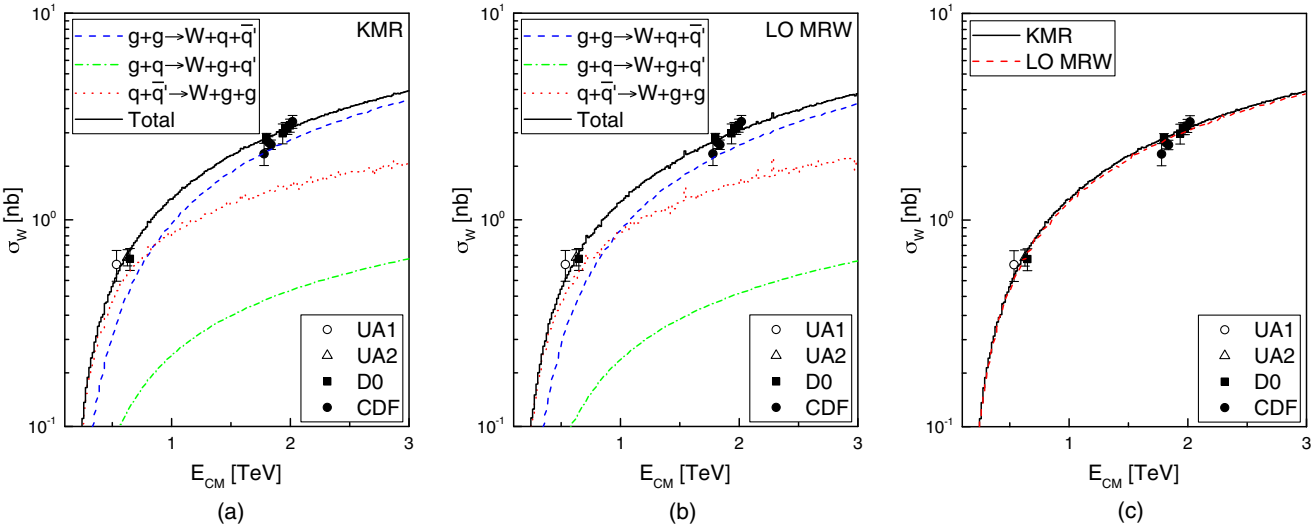

FIG. 15. The cross section of the production of the $W^{\pm}$ bosons as a function of the center-of-mass energy, E_{CM}. The experimental data are acquired from the UA1, UA2, D0, and CDF collaborations, Refs. [29–37]. The calculations are performed using the KMR and the LO MRW UPDF. We have omitted the NLO UPDF results here, to save computation data.

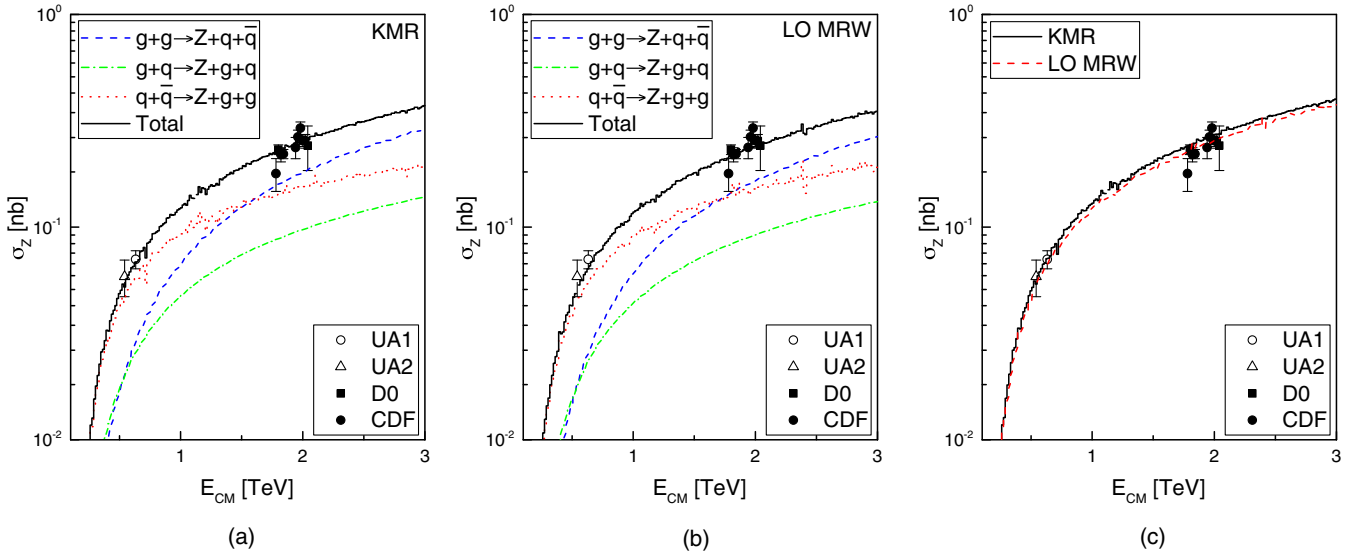

FIG. 16. The cross section of the production of the Z^0 bosons as a function of the center-of-mass energy, E_{CM}. The notation of the diagram is the same as in Fig. 15.

One should note that having a semisuccessful prediction from the framework of k_t factorization by itself is a success, since our calculations utilizing these UPDF inherently have a considerably larger error compared to those from the NNLO QCD or even the NLO QCD. This is because we are incorporating the single-scaled PDF (with their already included uncertainties) to form the double-scaled UPDF (or the triple-scaled DUPDF) with additional approximations and further uncertainties. Being able to provide predictions with a desirable accuracy would require a thorough universal fit for these frameworks; see Ref. [9]. The goal of these calculations is not to provide predictions that can exactly match the experimental data. We have performed these computations, merely to illustrate our point that the k_t factorization framework, despite its simplicity and computational advantages, can provide us with valuable insight regarding the transverse-momentum dependency of various high-energy QCD events.

In summary, within the present work, we have calculated the rate of productions belonging to the electroweak gauge

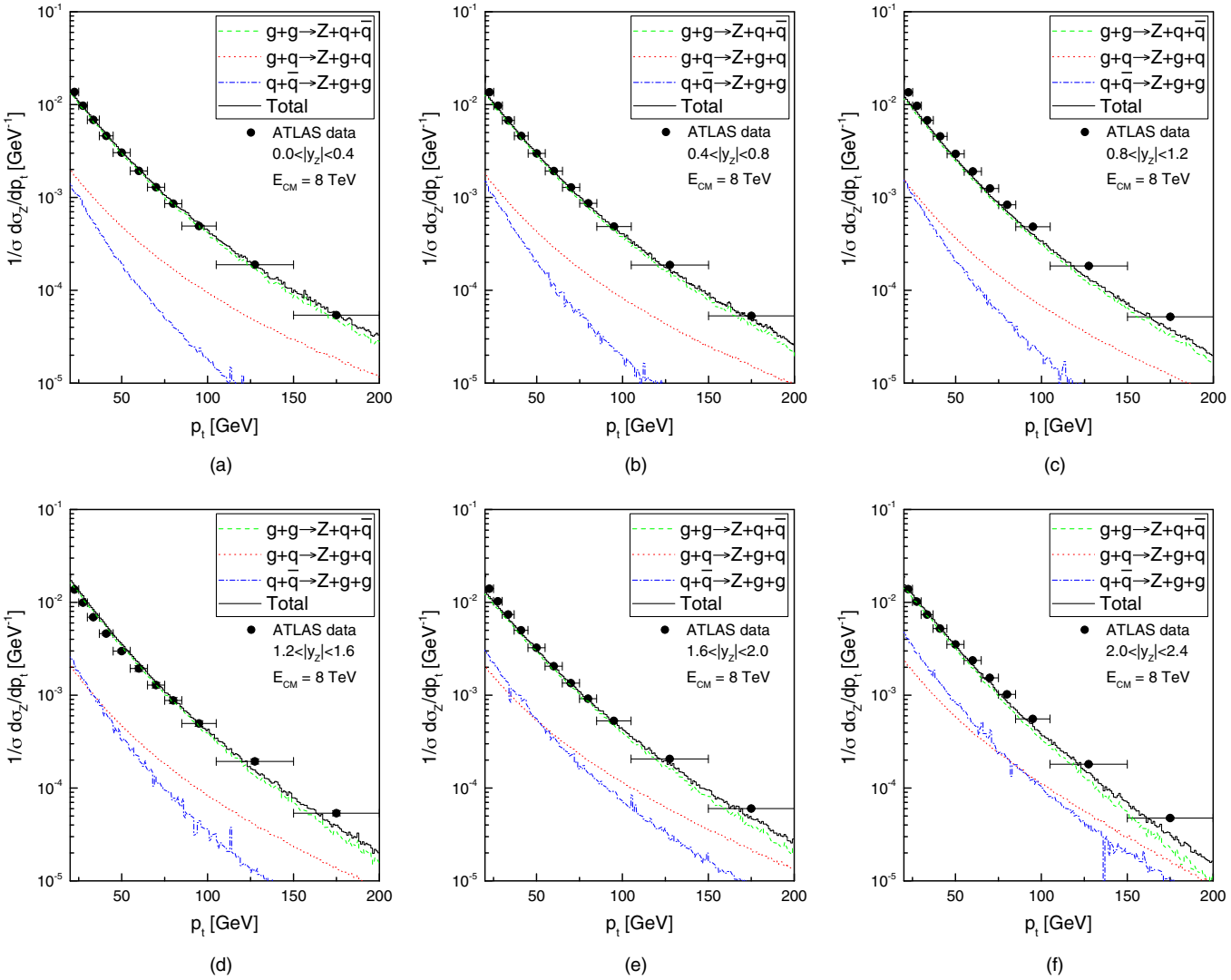

FIG. 17. (continued).

vector bosons in the framework of k_t factorization, utilizing the UPDF of KMR, LO mRW, and NLO MRW, by the means of NLO QCD processes. The results have been demonstrated and compared to each other and to the experimental data points from the D0 and the CDF collaborations, as well as the calculations in other frameworks. Through our analysis, we have suggested that, despite the theoretical advantages of the MRW, formalism, the KMR approach has better behavior toward describing the experiment. One can correctly argue that in the absence of uncertainty or ratio plots a precise comparison between the calculations and the experimental data is uneasy. However, it should be noted that including an accurate ratio plot would require developing an already proven baseline (e.g., a LO level Z^0 production in the k_t factorization or a NLO level in collinear factorization with the same resolution as of the original calculations) in addition to providing the original calculations with a decent uncertainty region (e.g., via manipulating the hard scale, μ, by a factor of 2). We will, however, try to address this shortcoming in our future work.

ACKNOWLEDGMENTS

M. M. would like to acknowledge the Research Council of University of Tehran and the Institute for Research and Planning in Higher Education for the grants provided for him. M. R. M. sincerely thanks A. Lipatov and N. Darvishi for their valuable discussions and comments. M. R. M. extends his gratitude toward his kind hosts at the Institute of Nuclear Physics, Polish Academy of Science, for their hospitality during his visit. He also acknowledges the Ministry of Science, Research and Technology of Iran that funded his visit.

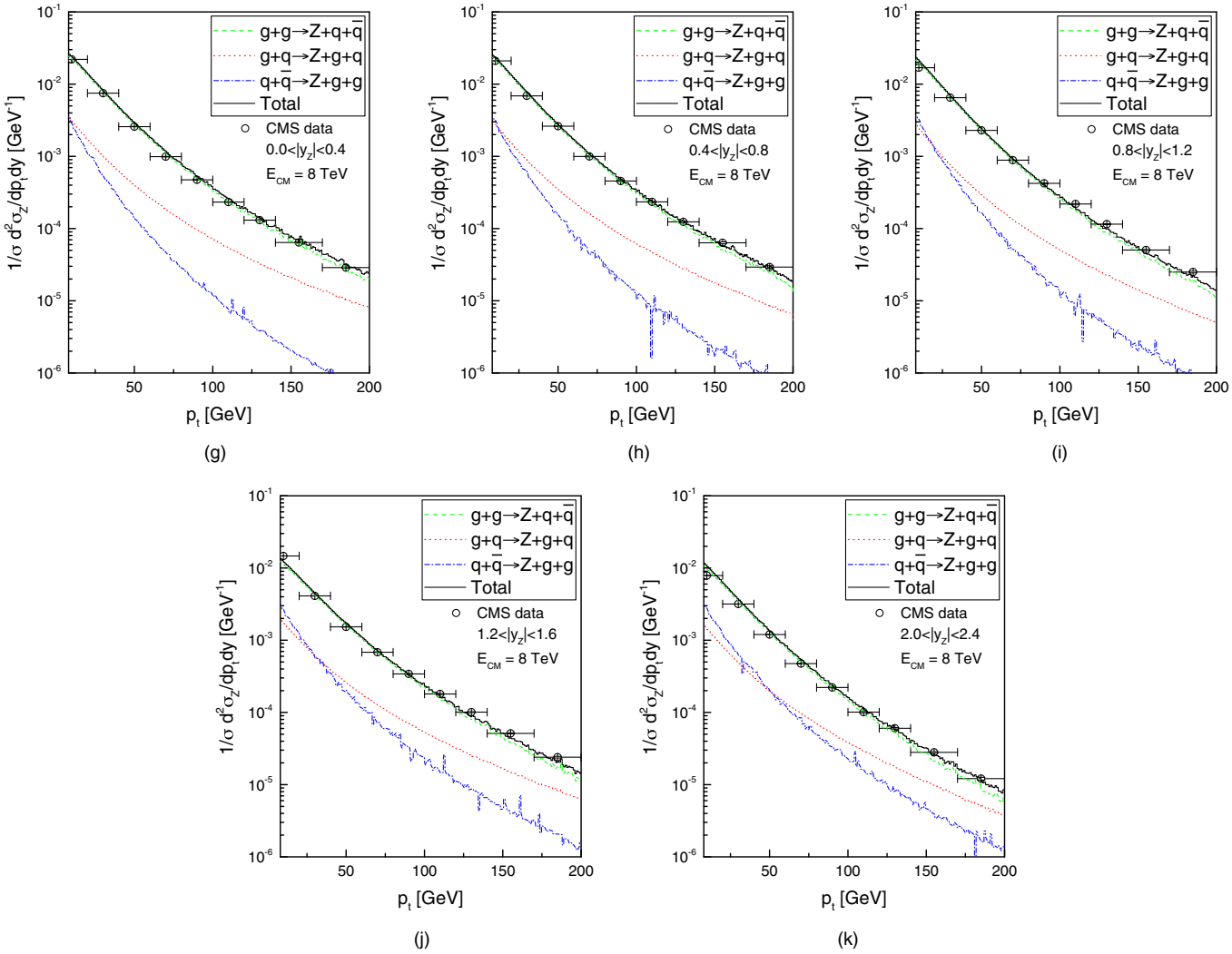

FIG. 17. Production of the Z^0 boson in $E_{\rm CM} = 8$ TeV, using the KMR approach. The individual contributions from the partonic subprocesses are presented, and the total values of (single and double) differential cross sections are subjected to comparison with the data of the ATLAS (black circles) and CMS (white circles) collaborations [38,39]. The labels (a) through (f) illustrate the results of our calculations for a single differential cross section of the production of Z^0, in the given rapidity regions. The results for double differential cross section are presented in the this figure with labels (g) through (h).

APPENDIX: THE MATRIX ELEMENTS OF THE PARTONIC SUBPROCESSES

Given that we are interested in the calculation of the matrix element squared for each process, one immediately concludes that the $|\mathcal{M}^{gg}|^2 = |\mathcal{M}^{qq}|^2$. Therefore, it is sufficient to calculate the invariant amplitudes for the Feynman diagrams of Fig. 2, the panels (b) and (c), which can be written as

$$\mathcal{M}^{ab} = \sum_{i=1}^{8} \mathcal{M}_i^{ab}, \qquad a, b = q, g, \tag{A1}$$

with

$$\mathcal{M}_1^{qg} = g_s^2 u(k_1) t^a \gamma_\mu \epsilon^\mu(p_1) \frac{\cancel{(k_1 - p_1)} + m}{(k_1 - p_1)^2 - m^2} G^\lambda_{W,Z} \epsilon_\lambda(p_3) \frac{\cancel{(k_2 + p_2)} + m}{(k_2 + p_2)^2 - m^2} t^b \gamma_\nu \epsilon^\nu(k_2) \bar{u}(p_2), \tag{A2}$$

$$\mathcal{M}_2^{qg} = g_s^2 u(k_1) t^b \gamma_\nu \epsilon^\nu(k_2) \frac{\cancel{(k_1 + k_2)} + m}{(k_1 + k_2)^2 - m^2} G^\lambda_{W,Z} \epsilon_\lambda(p_3) \frac{\cancel{(k_2 + k_2 - p_3)} + m}{(k_2 + k_2 - p_3)^2 - m^2} t^a \gamma_\mu \epsilon^\mu(p_1) \bar{u}(p_2), \tag{A3}$$

$$\mathcal{M}_3^{qg} = 2g_s^2 u(k_1) t^a \gamma_\mu \epsilon^\mu(p_1) \frac{\cancel{(k_1 - p_1)} + m}{(k_1 - p_1)^2 - m^2} t^b \gamma_\nu \epsilon^\nu(k_2) \frac{\cancel{(p_2 + p_3)} + m}{(p_2 + p_3)^2 - m^2} G^\lambda_{W,Z} \epsilon_\lambda(p_3) \bar{u}(p_2), \tag{A4}$$

$$\mathcal{M}_4^{qg} = 2g_s^2 u(k_1) t^a \gamma_\mu \epsilon^\mu(k_2) \frac{\cancel{(k_1 + k_2)} + m}{(k_1 + k_2)^2 - m^2} t^b \gamma_\nu \epsilon^\nu(p_1) \frac{\cancel{(k_1 + k_2 - p_1)} + m}{(k_1 + k_2 - p_1)^2 - m^2} G^\lambda_{W,Z} \epsilon_\lambda(p_3) \bar{u}(p_2), \tag{A5}$$

$$\mathcal{M}_5^{qg} = g_s^2 u(k_1) \gamma^\rho C^{\mu\nu\rho}(k_2, -p_1, p_1 - k_2) \frac{\epsilon_\mu \epsilon_\nu}{(k_2 - p_1)^2} f^{abc} t^c \frac{\cancel{(p_2 + p_3)} + m}{(p_2 + p_3)^2 - m^2} G^\lambda_{W,Z} \epsilon_\lambda(p_3) \bar{u}(p_2), \tag{A6}$$

$$\mathcal{M}_6^{qg} = g_s^2 u(k_1) G^\lambda_{W,Z} \epsilon_\lambda(p_3) \frac{\cancel{(k_1 - p_3)} + m}{(k_1 - p_3)^2 - m^2} \gamma^\rho C^{\mu\nu\rho}(k_2, -p_1, p_1 - k_2) \frac{\epsilon_\mu \epsilon_\nu}{(k_2 - p_1)^2} f^{abc} t^c \bar{u}(p_2), \tag{A7}$$

and

$$\mathcal{M}_1^{gg} = g_s^2 \bar{u}(p_1) t^a \gamma_\mu \epsilon^\mu(k_1) \frac{\cancel{(p_1 - k_1)} + m}{(p_1 - k_1)^2 - m^2} G^\lambda_{W,Z} \epsilon_\lambda(p_3) \frac{\cancel{(p_2 + k_2)} + m}{(p_2 + k_2)^2 - m^2} t^b \gamma_\nu \epsilon^\nu(k_2) u(p_2), \tag{A8}$$

$$\mathcal{M}_2^{gg} = g_s^2 \bar{u}(p_1) t^a \gamma_\mu \epsilon^\mu(k_1) \frac{\cancel{(k_2 - p_1)} + m}{(k_2 - p_1)^2 - m^2} G^\lambda_{W,Z} \epsilon_\lambda(p_3) \frac{\cancel{(k_1 + p_2)} + m}{(k_1 + p_2)^2 - m^2} t^b \gamma_\nu \epsilon^\nu(k_2) u(p_2), \tag{A9}$$

$$\mathcal{M}_3^{gg} = g_s^2 \bar{u}(p_1) \frac{\cancel{(p_1 + p_3)} + m}{(p_1 + p_3)^2 - m^2} t^a \gamma_\mu \epsilon^\mu(k_1) \frac{\cancel{(p_1 + p_3 - k_1)} + m}{(p_1 + p_3 - k_1)^2 - m^2} G^\lambda_{W,Z} \epsilon_\lambda(p_3) t^b \gamma_\nu \epsilon^\nu(k_2) u(p_2), \tag{A10}$$

$$\mathcal{M}_4^{gg} = g_s^2 \bar{u}(p_1) G^\lambda_{W,Z} \epsilon_\lambda(p_3) t^a \gamma_\mu \epsilon^\mu(k_1) \frac{\cancel{(p_1 - k_1)} + m}{(p_1 - k_1)^2 - m^2} t^b \gamma_\nu \epsilon^\nu(k_2) \frac{\cancel{(p_1 - k_1 - k_2)} + m}{(p_1 - k_1 - k_2)^2 - m^2} u(p_2), \tag{A11}$$

$$\mathcal{M}_5^{gg} = g_s^2 \bar{u}(p_1) G^\lambda_{W,Z} \epsilon_\lambda(p_3) \frac{\cancel{(p_1 + p_3)} + m}{(p_1 + p_3)^2 - m^2} t^b \gamma_\nu \epsilon^\nu(k_2) \frac{\cancel{(p_1 + p_3 - k_2)} + m}{(p_1 + p_3 - k_2)^2 - m^2} t^a \gamma_\mu \epsilon^\mu(k_1) u(p_2), \tag{A12}$$

$$\mathcal{M}_6^{gg} = g_s^2 \bar{u}(p_1) G^\lambda_{W,Z} \epsilon_\lambda(p_3) t^b \gamma_\nu \epsilon^\nu(k_2) \frac{\cancel{(p_1 - k_2)} + m}{(p_1 - k_2)^2 - m^2} t^a \gamma_\mu \epsilon^\mu(k_1) \frac{\cancel{(p_1 - k_1 - k_2)} + m}{(p_1 - k_1 - k_2)^2 - m^2} u(p_2), \tag{A13}$$

$$\mathcal{M}_7^{gg} = g_s^2 \bar{u}(p_1) \gamma^\rho C^{\mu\nu\rho}(k_1, k_2, -k_1 - k_2) \frac{\epsilon_\mu \epsilon_\nu}{(k_1 + k_2)^2} f^{abc} t^c \frac{\cancel{(p_1 - k_1 - k_2)} + m}{(p_1 - k_1 - k_2)^2 - m^2} G^\lambda_{W,Z} \epsilon_\lambda(p_3) u(p_2), \tag{A14}$$

$$\mathcal{M}_8^{gg} = g_s^2 \bar{u}(p_1) G^\lambda_{W,Z} \epsilon_\lambda(p_3) \frac{\cancel{(p_1 - p_3)} + m}{(p_1 - p_3)^2 - m^2} \gamma^\rho C^{\mu\nu\rho}(k_1, k_2, -k_1 - k_2) \frac{\epsilon_\mu \epsilon_\nu}{(k_1 + k_2)^2} f^{abc} t^c u(p_2), \tag{A15}$$

where g_s is the running coupling constant for QCD and $G^\lambda_{W,Z}$ represents the vertex of the electroweak gauge vector bosons with quarks:

$$\begin{aligned} G^\lambda_W &= \frac{e_{\rm em}}{2\sqrt{2}\sin\theta_w} \gamma^\lambda (1 - \gamma^5) V_{qq'} \\ G^\lambda_Z &= \frac{e_{\rm em}}{\sin 2\theta_w} \gamma^\lambda [I_{3,q}(1 - \gamma^5) - 2e_q \sin^2\theta_w]. \end{aligned} \tag{A16}$$

θ_w is the Weinberg angle, $V_{qq'}$ is the corresponding CKM matrix element, and $I_{3,q}$ is the weak isospin component of the quark q. Additionally, the standard QCD three-gluon coupling can be written as follows:

$$C^{\mu\nu\rho}(k_1, k_2, k_3) = g^{\mu\nu}(k_2 - k_1)^\rho + g^{\nu\rho}(k_3 - k_2)^\mu + g^{\rho\mu}(k_1 - k_3)^\nu. \tag{A17}$$

With the above information, one has enough tools to calculate the matrix elements of Eq. (25).

[1] V. N. Gribov and L. N. Lipatov, Yad. Fiz. **15**, 781 (1972).
[2] L. N. Lipatov, Sov. J. Nucl. Phys. **20**, 94 (1975).
[3] G. Altarelli and G. Parisi, Nucl. Phys. **B126**, 298 (1977).
[4] Y. L. Dokshitzer, Sov. Phys. JETP **46**, 641 (1977).
[5] M. A. Kimber, A. D. Martin, and M. G. Ryskin, Phys. Rev. D **63**, 114027 (2001).
[6] A. D. Martin, M. G. Ryskin, and G. Watt, Eur. Phys. J. C **66**, 163 (2010).
[7] M. A. Kimber, J. Kwiecinski, A. D. Martin, and A. M. Stasto, Phys. Rev. D **62**, 094006 (2000).
[8] M. A. Kimber, Ph.D. thesis, University of Durham, 2001.
[9] G. Watta, A. D. Martina, and M. G. Ryskina, Phys. Rev. D **70**, 014012 (2004).
[10] M. Ciafaloni, Nucl. Phys. **B296**, 49 (1988).
[11] S. Catani, F. Fiorani, and G. Marchesini, Phys. Lett. B **234**, 339 (1990).
[12] S. Catani, F. Fiorani, and G. Marchesini, Nucl. Phys. **B336**, 18 (1990).
[13] M. G. Marchesini, *Proceedings of the Workshop QCD at 200 TeV, Erice, Italy*, edited by L. Cifarelli and Yu. L. Dokshitzer (Plenum, New York, 1992), p. 183.
[14] G. Marchesini, Nucl. Phys. **B445**, 49 (1995).
[15] J. Kwiecinski, A. D. Martin, and P. J. Sutton, Phys. Rev. D **52**, 1445 (1995).
[16] V. S. Fadin, E. A. Kuraev, and L. N. Lipatov, Phys. Lett. B **60**, 50 (1975).
[17] L. N. Lipatov, Sov. J. Nucl. Phys. **23**, 642 (1976).
[18] E. A. Kuraev, L. N. Lipatov, and V. S. Fadin, Sov. Phys. JETP **44**, 45 (1976).
[19] E. A. Kuraev, L. N. Lipatov, and V. S. Fadin, Sov. Phys. JETP **45**, 199 (1977).
[20] Ya. Ya. Balitsky and L. N. Lipatov, Sov. J. Nucl. Phys. **28**, 822 (1978).
[21] M. Modarres and H. Hosseinkhani, Nucl. Phys. **A815**, 40 (2009).
[22] M. Modarres and H. Hosseinkhani, Few-Body Syst. **47**, 237 (2010).
[23] H. Hosseinkhani and M. Modarres, Phys. Lett. B **694**, 355 (2011).
[24] H. Hosseinkhani and M. Modarres, Phys. Lett. B **708**, 75 (2012).
[25] M. Modarres, H. Hosseinkhani, and N. Olanj, Nucl. Phys. **A902**, 21 (2013).
[26] M. Modarres, H. Hosseinkhani, and N. Olanj, Phys. Rev. D **89**, 034015 (2014).
[27] M. Modarres, H. Hosseinkhani, N. Olanj, and M. R. Masouminia, Eur. Phys. J. C **75**, 556 (2015).
[28] M. Modarres, M. R. Masouminia, H. Hosseinkhani, and N. Olanj, Nucl. Phys. **A945**, 168185 (2016).
[29] C. Albajar *et al.* (UA1 Collaboration), Phys. Lett. B **253**, 503 (1991).
[30] J. Alitti *et al.* (UA2 Collaboration), Z. Phys. **47**, 11 (1990).
[31] F. Abe *et al.* (CDF Collaboration), Phys. Rev. Lett. **76**, 3070 (1996).
[32] B. Affolder *et al.* (CDF Collaboration), Phys. Rev. Lett. **84**, 845 (2000).
[33] S. Abachi *et al.* (D0 Collaboration), Phys. Rev. Lett. **75**, 1456 (1995).
[34] B. Abbott *et al.* (D0 Collaboration), Phys. Rev. Lett. **80**, 5498 (1998).
[35] B. Abbott *et al.* (D0 Collaboration), Phys. Rev. D **61**, 072001 (2000).
[36] B. Abbott *et al.* (D0 Collaboration), Phys. Rev. D **61**, 032004 (2000).
[37] B. Abbott *et al.* (D0 Collaboration), Phys. Lett. B **513**, 292 (2001).
[38] S. I. Godunov, A. N. Rozanov, M. I. Vysotsky, and E. V. Zhemchugov (ATLAS Collaboration), Eur. Phys. J. C **76**, 1 (2016).
[39] V. Khachatryan *et al.* (CMS Collaboration), Phys. Lett. B **749**, 187 (2015).
[40] S. P. Baranov, A. V. Lipatov, and N. P. Zotov, Phys. Rev. D **78**, 014025 (2008).
[41] M. Deak, Ph.D. thesis, University of Hamburg, 2009.
[42] A. Gehrmann-De Ridder, T. Gehrmann, E. W. N. Glover, A. Huss, and T. A. Morgan, J. High Energy Phys. 07 (2016) 133.
[43] A. D. Martin, W. J. Stirling, R. S. Thorne, and G. Watt, Eur. Phys. J. C **63**, 189 (2009).
[44] A. D. Martin, W. J. Stirling, R. S. Thorne, and G. Watt, Eur. Phys. J. C **64**, 653 (2009).
[45] A. D. Martin, W. J. Stirling, R. S. Thorne, and G. Watt, Eur. Phys. J. C **70**, 51 (2010).
[46] L. A. Harland-Lang, A. D. Martin, P. Motylinski, and R. S. Thorne, Eur. Phys. J. C **75**, 204 (2015).
[47] J. Kwiecinski, A. D. Martin, and A. M. Stasto, Phys. Rev. D **56**, 3991 (1997).
[48] K. Golec-Biernat and A. M. Stasto, Phys. Rev. D **80**, 014006 (2009).
[49] G. Watt, Ph.D. thesis, University of Durham, 2004.
[50] M. A. Kimber, A. D. Martin, and M. G. Ryskin, Eur. Phys. J. C **12**, 655 (2000).
[51] W. Furmanski and R. Petronzio, Phys. Lett. B **97**, 437 (1980).
[52] S. P. Baranov, A. V. Lipatov, and N. P. Zotov, Phys. Rev. D **81**, 094034 (2010).
[53] A. V. Lipatov and N. P. Zotov, Phys. Rev. D **81**, 094027 (2010); **72**, 054002 (2005).
[54] J. A. M. Vermaseren, *Symbolic Manipulation with FORM* (Computer Algebra, Kruislaan, Netherlands, 1991), 413, 1098, SJ Amsterdaam.
[55] M. Cacciari, G. P. Salam, and G. Soyez, J. High Energy Phys. 04 (2008) 063.
[56] W.-M. Yao *et al.* (Particle Data Group Collaboration), J. Phys. G **33**, 1 (2006).
[57] P. Jimenez-Delgado and E. Reya, Phys. Rev. D **79**, 074023 (2009).
[58] M. Glck and E. Reya, Mod. Phys. Lett. A **22**, 351 (2007).
[59] P. Jimenez-Delgado and E. Reya, Phys. Rev. D **80**, 114011 (2009).